STING mediates immune responses in a unicellular choanoflagellate

Arielle Woznica[1*], Ashwani Kumar[2], Carolyn R. Sturge[1], Chao Xing[2], Nicole King[3], Julie K. Pfeiffer[1*]

[1] Department of Microbiology, University of Texas Southwestern Medical Center, Dallas TX 75390, USA
[2] McDermott Center Bioinformatics Lab, University of Texas Southwestern Medical Center, Dallas TX, USA
[3] Howard Hughes Medical Institute, and Department of Molecular and Cell Biology, University of California, Berkeley, Berkeley, CA 94720, USA.

*Correspondence: Arielle.Woznica@UTSouthwestern.edu and Julie.Pfeiffer@UTSouthwestern.edu

Abstract

Animals have evolved unique repertoires of innate immune genes and pathways that provide their first line of defense against pathogens. To reconstruct the ancestry of animal innate immunity, we have developed the choanoflagellate *Monosiga brevicollis*, one of the closest living relatives of animals, as a model for studying mechanisms underlying pathogen recognition and immune response. We found that *M. brevicollis* is killed by exposure to *Pseudomonas aeruginosa* bacteria and selectively avoids ingesting them. Moreover, *M. brevicollis* expresses STING, which, in animals, activates innate immune pathways in response to cyclic dinucleotides during pathogen sensing. *M. brevicollis* STING increases the susceptibility of *M. brevicollis* to *P. aeruginosa*-induced cell death and is required for responding to the cyclic dinucleotide 2'3' cGAMP. Furthermore, similar to animals, autophagic signaling in *M. brevicollis* is induced by 2'3' cGAMP in a STING-dependent manner. This study provides evidence for a pre-animal role for STING in antibacterial immunity and establishes *M. brevicollis* as a model system for the study of immune responses.

Introduction

Innate immunity is the first line of defense against pathogens for all animals, in which it is crucial for distinguishing between self and non-self, recognizing and responding to pathogens, and repairing cellular damage. Some mechanisms of animal immunity have likely been present since the last common eukaryotic ancestor, including RNAi, production of antimicrobial peptides, and the production of nitric oxide[1,2]. However, many gene families that play critical roles in animal innate immune responses are unique to animals[3].

Comparing animals with their closest relatives, the choanoflagellates, can provide unique insights into the ancestry of animal immunity and reveal other key features of the first animal, the 'Urmetazoan'[4–6]. Choanoflagellates are microbial eukaryotes that live in diverse aquatic environments and survive by capturing and phagocytosing diverse environmental bacteria[7] using their "collar complex," an apical flagellum surrounded by actin-filled microvilli (Fig. 1A)[7,8]. Several innate immune pathway genes once considered to be animal-specific are present in choanoflagellates, including cGAS and STING, both of which are crucial for innate responses to cytosolic DNA in animals (Fig. S1)[3,9,10]. Although the phylogenetic distribution of these gene families reveals that they first evolved before animal origins, their functions in choanoflagellates and their contributions to the early evolution of animal innate immunity are unknown.

STING (stimulator of interferon genes) is a signaling protein that activates innate immune responses to cytosolic DNA during bacterial or viral infection[11,12]. Although STING homologs are conserved in diverse invertebrate and vertebrate animals (reviewed in Margolis et al. 2017)[9,13,14], mechanisms of STING activation are best understood in mammals. In mammals, STING is activated by binding 2'3' cGAMP, an endogenous cyclic dinucleotide produced by the sensor cGAS (cyclic GMP-AMP synthase) upon detecting cytosolic DNA[15–20.]. In addition, cyclic dinucleotides produced by bacteria can also activate STING[17,21]. Importantly, STING domain-containing systems are present in bacteria, and eukaryotic STING-like proteins may have been acquired from lateral gene transfer[22]. Comparative genomics suggests that STING domains arose at least three independent times in eukaryotes, including once in the stem lineage leading to Choanozoa, the clade containing animals and choanoflagellates[22].

Choanoflagellates have already served as powerful models for studying the origin of animal multicellularity and cell differentiation[10,23–28] and are ideally positioned to yield insights into the evolution of animal immune pathways. Therefore, we sought to establish the choanoflagellate *Monosiga brevicollis* as a model for studying pathogen recognition and immune responses. Here, we report that *Pseudomonas aeruginosa* bacteria are pathogenic for *M. brevicollis.* Through our study of interactions between *P.*

aeruginosa and *M. brevicollis*, we determine that STING functions in the choanoflagellate antibacterial response. In addition, we demonstrate that STING is necessary for mediating responses to the STING agonist 2'3' cGAMP *in vivo*, and that 2'3' cGAMP induces STING-dependent autophagic signaling. Our results demonstrate that key features of STING-mediated immune responses are conserved in *M. brevicollis*, thereby expanding our understanding of the pre-metazoan ancestry of STING signaling.

Results

P. aeruginosa has pathogenic effects on *M. brevicollis*

One impediment to studying immune responses in choanoflagellates has been the lack of known choanoflagellate pathogens. While bacteria are obligate prey and can regulate mating, multicellular development, and cell contractility in choanoflagellates, to our knowledge no bacteria with pathogenic effects have been described [23,26,27,29–31]. For this study, we focused on the choanoflagellate *Monosiga brevicollis,* which has a sequenced genome[4], grows robustly under laboratory conditions in co-culture with *Flavobacterium* prey bacteria[5], and expresses a clear homolog of STING[3,9]. To identify potential pathogens of choanoflagellates, we screened select bacteria – including environmental isolates and known animal pathogens and commensals (Table 1) – to test whether any of these induced *M. brevicollis* behavioral changes or reduced cell survival.

After co-culturing *M. brevicollis* with bacteria for 24 hours, only the gammaproteobacterium *Pseudomonas aeruginosa,* a ubiquitous environmental bacterium and opportunistic pathogen of diverse eukaryotes[32–35], altered the behavior and growth dynamics of *M. brevicollis*. Under standard laboratory conditions, *M. brevicollis* is a highly motile flagellate and swims up in the water column (Movie 1). However, after 12-14 hours in the presence of *P. aeruginosa* strains PAO1 and PA14, a large proportion of *M. brevicollis* cells settled to the bottom of the culture dish (Movie 2). Immunofluorescence staining revealed that *M. brevicollis* cells exposed to *P. aeruginosa* had truncated flagella compared to cells exposed to *E. coli* or other bacteria that did not induce cell settling (Fig. 1B). To determine the effects of *P. aeruginosa* on cell viability, we added *P. aeruginosa* strain PAO1 or control gammaproteobacteria to *M. brevicollis* and monitored cell density over the course of 72 hours (Fig. 1C). While *M. brevicollis* continued to proliferate in the presence of control gammaproteobacteria, exposure to *P. aeruginosa* PAO1 resulted in cell death.

Choanoflagellates prey upon bacteria and ingest them through phagocytosis[7,8]. However, many bacterial pathogens have evolved strategies to prevent or resist phagocytosis by eukaryotic cells[36,37]. Therefore, we examined whether exposure to *P.*

aeruginosa alters *M. brevicollis* phagocytic uptake. To track phagocytosis, we added GFP-expressing *E. coli* DH5α (Fig. 1D) or *P. aeruginosa* PAO1 (Fig. 1E) to *M. brevicollis* and monitored the cultures by live imaging. After one hour, while 92% of *M. brevicollis* cells incubated with *E. coli*–GFP had GFP+ food vacuoles, only 3% of cells incubated with PAO1-GFP had GFP+ food vacuoles (Fig. 1F).

Next, to determine if *P. aeruginosa* broadly disrupts *M. brevicollis* phagocytosis or if *M. brevicollis* specifically avoids ingestion of *P. aeruginosa*, we incubated *M. brevicollis* with GFP-expressing PAO1 or GFP-expressing *E. coli* for one hour, and then added 0.2 mm fluorescent beads for an additional 30 minutes as an independent measure of phagocytic activity. The fraction of *M. brevicollis* cells with internalized 0.2 mm beads was similar in cultures incubated with *E. coli* DH5α and PAO1 (Fig. 1G). Moreover, exposure to *P. aeruginosa* did not inhibit phagocytic uptake of *E. coli* (Fig. 1H). These results suggest that exposure to *P. aeruginosa* does not broadly alter phagocytosis, but rather that *M. brevicollis* specifically avoids ingesting *P. aeruginosa*.

We next investigated the effects of secreted *P. aeruginosa* molecules on *M. brevicollis* viability. Exposure of *M. brevicollis* to conditioned medium from *P. aeruginosa* PAO1 or diverse non-pathogenic gammaproteobacteria revealed that PAO1 conditioned medium is sufficient to induce cell death (Fig. 1I). Similar to live bacteria, exposure to *P. aeruginosa* conditioned medium led to reduced motility and truncated flagella in *M. brevicollis* after approximately 10 hours. Because numerous *P. aeruginosa* secreted virulence factors have been characterized[32,38], we screened a battery of isogenic PAO1 strains with deletions in known virulence genes to determine if any of these factors contribute to the pathogenic effects on *M. brevicollis* (Table 2). All strains tested induced similar levels of *M. brevicollis* cell death as the parental PAO1 strain, suggesting that none of the deleted virulence genes alone are essential for pathogenesis in *M. brevicollis*. These results suggest that other *P. aeruginosa* virulence factors are required for inducing cell death in *M. brevicollis.*

Upregulation of *M. brevicollis* STING in response to *P. aeruginosa*

To identify potential genetic pathways activated by *M. brevicollis* in response to pathogenic bacteria, we performed RNA-seq on *M. brevicollis* exposed to conditioned medium from either *P. aeruginosa* or *Flavobacterium sp*., the non-pathogenic bacterial strain used as a food source (Table 1). We found that 674 genes were up-regulated and 232 genes were downregulated two-fold or greater (FDR≤10^{-4}) upon *P. aeruginosa* exposure compared to cells exposed to *Flavobacterium* (Fig. 2A). The up-regulated genes were enriched in biological processes including response to stress, endocytosis, microtubule-based movement, mitochondrial fission, and carbohydrate metabolism. Genes down-regulated in response to *P. aeruginosa* were enriched in biological processes including RNA modification and metabolism (Fig. S2A). We also found that

the transcription of several genes encoding proteins that function in animal antibacterial innate immunity was upregulated in response to *P. aeruginosa*, including C-type lectin, glutathione peroxidase, and STING (Fig. 2A,B). Using an antibody we raised against the C-terminal portion of *M. brevicollis* STING (Fig. S2B) we found that STING protein levels are also elevated in response to *P. aeruginosa* (Fig. 2C). Given the importance of STING in animal immunity and its upregulation in response to *P. aeruginosa*, we pursued its functional relevance in the *M. brevicollis* pathogen response.

The cyclic dinucleotide 2'3' cGAMP induces elevated expression of STING in *M. brevicollis*

The predicted domain architecture of *M. brevicollis* STING consists of four transmembrane domains followed by a cytosolic STING domain (Fig. 3A, Fig. S2C), and likely matches the structure of the ancestral animal STING protein. Vertebrate STING proteins contain a C-terminal tail (CTT; Fig. 3A, Fig. S2C) that is required for the induction of interferons[39–41], and for the activation of other downstream responses, including NFkB[42] and autophagy[43–45] pathways. Both the STING CTT and interferons evolved in vertebrates and it is currently unclear how choanoflagellate and invertebrate STING proteins mediate downstream immune responses[13,46]. The conservation of putative cyclic dinucleotide-binding residues in *M. brevicollis* STING (Fig. 3B) led us to hypothesize that *P. aeruginosa* could induce STING by producing bacterial cyclic dinucleotides[12,17,21]. In addition, because *M. brevicollis* has a cGAS-like enzyme (Fig. S1A), it is also possible that *P. aeruginosa* exposure could lead to the production of an endogenous cyclic dinucleotide[9,12,47].

To identify potential STING inducers[49,50], we treated *M. brevicollis* with purified immune agonists, including mammalian cGAMP (2'3' cGAMP) and bacterial cyclic dinucleotides (3'3' c-di-GMP, 3'3' c-di-AMP, 3'3' cGAMP). We first performed dose-response curves to determine if the different cyclic dinucleotides affect the viability of *M. brevicollis* (Fig. 3C). Interestingly, we found that exposure to 2'3' cGAMP induced cell death in a dose-dependent manner. In contrast, exposure to 3'3' cGAMP, c-di-GMP, and c-di-AMP did not alter *M. brevicollis* survival. Transcriptional profiling of *M. brevicollis* exposed to 2'3' cGAMP or 3'3' cGAMP for three hours revealed that *STING* mRNA levels increase in response to 2'3' cGAMP, but remain unchanged in response to 3'3cGAMP (Fig. S3A-C). Therefore, we next treated *M. brevicollis* with the cyclic dinucleotides for five hours, and measured STING protein levels by immunoblot (Fig. 3D). Treatment with 2'3' cGAMP, but not the bacterially-produced cyclic dinucleotides, led to elevated levels of STING protein compared to unstimulated cells. A time course of 2'3' cGAMP treatment revealed that STING protein levels increase as early as three hours after exposure to the cyclic dinucleotide and remain elevated for at least 7 hours, approximately one cell cycle (Fig. 3E). While we also observed sustained upregulation

of STING in the presence of *P. aeruginosa*, this is markedly different from what has been described in mammals, wherein STING activation results in its translocation to lysosomes and degradation[45]. In addition, immunostaining for STING in fixed *M. brevicollis* revealed that the number and intensity of STING puncta increases after exposure to 2'3' cGAMP (Fig. S3E,F). These data suggest that *M. brevicollis* STING responds to 2'3' cGAMP, and that this cyclic dinucleotide can be used to further characterize the role of STING in *M. brevicollis*.

Transfection reveals that STING localizes to the *M. brevicollis* endoplasmic reticulum

A key barrier to investigating gene function in *M. brevicollis* has been the absence of transfection and reverse genetics. We found that the transfection protocol recently developed for the choanoflagellate *Salpingoeca rosetta*[48] was not effective in *M. brevicollis*, but by implementing a number of alterations to optimize reagents and conditions (see Methods) we were able to achieve both reproducible transfection and establishment of stable cell lines in *M. brevicollis*.

To investigate the subcellular localization of STING, we established a robust transfection protocol for *M. brevicollis* that would allow the expression of fluorescently-labeled STING along with fluorescent subcellular markers for different organelles. We observed that STING-mTFP protein localized to tubule-like structures around the nucleus (Fig. 4A) similar to what was observed by immunostaining with an antibody to STING (Fig. S3E,F). We then co-transfected STING-mTFP alongside fluorescent reporters marking the endoplasmic reticulum (ER) or mitochondria (Fig. 4B,C) and performed live-cell imaging. STING-mTFP co-localized with a fluorescent marker highlighting the ER (Fig. 4B). Thus, as in mammalian cells[15,49], STING localizes to regions of the ER in *M. brevicollis*.

Genetic disruption of STING reveals its role in responding to 2'3' cGAMP and *P. aeruginosa*

The establishment of transfection facilitated genome editing in *M. brevicollis*. Disrupting the *STING* locus using CRISPR/Cas9-mediated genome editing (Fig. 5A) enabled us to investigate the function of STING. To overcome low gene editing efficiencies in *M. brevicollis,* we based our gene editing strategy on a protocol recently developed for *S. rosetta* that simultaneously edits a gene of interest and confers cycloheximide resistance[50]. By selecting for cycloheximide resistance and then performing clonal isolation, we were able to isolate a clonal cell line that has a deletion within the *STING* locus that introduces premature stop codons (Fig. S5A). We were unable to detect STING protein in *STING*$^{-}$ cells by immunoblot (Fig. 5B). Wild type and

STING^{-} cells have similar growth kinetics (Fig. S5B), suggesting that STING is not required for cell viability under standard laboratory conditions. In addition, overexpression of STING-mTFP did not affect *M. brevicollis* viability.

To investigate the connection between 2'3' cGAMP and STING signaling in *M. brevicollis*, we exposed *STING*$^{-}$ cells to increasing concentrations of 2'3' cGAMP. In contrast to wild type *M. brevicollis*, *STING*$^{-}$ cells are resistant to 2'3' cGAMP-induced cell death (Fig. 5C). The 2'3' cGAMP resistance phenotype could be partially reversed by stably expressing STING within the *STING*$^{-}$ mutant background (Fig. 5D). In addition, *STING*$^{-}$ cells fail to induce a strong transcriptional response to 2'3' cGAMP compared to wild type cells (Fig. 5E, Fig. S3A, Fig. S5C,D). While 371 genes are differentially expressed in wild type cells after exposure to 2'3' cGAMP for three hours, only 28 genes are differentially expressed in *STING*$^{-}$ cells (FC ≥3; FDR≤10^{-4}). Thus, 2'3' cGAMP induces a STING-dependent transcriptional response in *M. brevicollis*.

Interestingly, of the 22 choanoflagellate species with sequenced transcriptomes[3,27], only *M. brevicollis* and *Salpingoeca macrocollata*, express homologs of both STING and cGAS (Fig. S1A, Fig. 5F, Fig. S5E). Therefore, we were curious whether other choanoflagellate species are able to respond to 2'3' cGAMP in the absence of a putative STING protein. We exposed four other choanoflagellate species (*Salpingoeca infusionum*, *S. macrocollata, S. rosetta*, and *Salpingoeca punica*) to increasing 2'3' cGAMP concentrations, and quantified survival after 24 hours (Fig. 5G). Of these additional species, only *S. macrocollata* had impaired survival in the presence of 2'3' cGAMP. Thus, it is possible that STING also responds to 2'3' cGAMP in *S. macrocollata.*

We next asked whether *STING*$^{-}$ cells have altered responses to other immune agonists. Although *M. brevicollis* is continuously co-cultured with feeding bacteria, we observed that treatment with high concentrations of *E. coli* lipopolysaccharides induces cell death (Fig. S5F). As LPS is not known to activate STING signaling, we treated wild type and *STING*$^{-}$ cells with LPS to probe the specificity of STING-mediated immune responses in *M. brevicollis*. The survival responses of wild type and *STING*$^{-}$ cells to LPS were indistinguishable (Fig. 5H), suggesting that there are separable pathways for responding to 2'3' cGAMP and LPS. We also examined the survival of *STING*$^{-}$ cells exposed to *P. aeruginosa* conditioned medium (Fig. 5I, Fig. S5G). In growth curve experiments, *P. aeruginosa* hindered the growth rate and stationary phase cell density of *STING*$^{-}$ cells compared to *Flavobacterium* (Fig. S5G). However, *STING*$^{-}$ cells were still able to divide in the presence of *P. aeruginosa,* whereas wild type cell growth was completely restricted (Figure 5I). These results indicate that wild type cells are more susceptible to *P. aeruginosa* than *STING*$^{-}$ cells, although it is unclear how STING contributes to *P. aeruginosa*-induced growth restriction and cell death.

2'3' cGAMP-induces autophagic signaling via STING

One downstream consequence of STING signaling in animals is the initiation of autophagy[21,43,44,47,51]. Based on viral infection studies in *D. melanogaster*[51] and experiments expressing invertebrate STING in mammalian cells[43], it has been proposed that the induction of autophagy may be an interferon-independent 'ancestral' function of STING. Although *M. brevicollis* lacks many effectors required for immune responses downstream of STING in animals (including TBK1 and NF-kB; Figure S1A), autophagy machinery is well conserved in *M. brevicollis*. Therefore, we asked if one outcome of 2'3' cGAMP exposure in *M. brevicollis* is the induction of autophagy.

The evolutionarily conserved protein Atg8/LC3 is a ubiquitin-like protein that can be used to monitor autophagy[52,53]. During autophagosome formation, unmodified Atg8, called Atg8-I, is conjugated to phosphatidylethanolamine. Lipidated Atg8, called Atg8-II, remains associated with growing autophagosomes. As such, two indicators of autophagy are elevated Atg8-II levels relative to Atg8-I and increased formation of Atg8+ autophagosome puncta. Because antibodies are not available to detect endogenous *M. brevicollis* autophagy markers or cargo receptors, we generated wild type and *STING*$^{-}$ cell lines stably expressing mCherry-Atg8. Expression of mCherry-Atg8 did not alter the relative susceptibilities of these cell lines to 2'3'cGAMP (Fig. S6A). By immunoblot, mCherry-Atg8-II can be distinguished from mCherry-Atg8-I based on its enhanced gel mobility. When we exposed both cell lines to 2'3' cGAMP for three hours, we observed increased levels of Atg8-II relative to Atg8-I by immunoblot in wild type, but not *STING*$^{-}$ cells (Fig. 6A). These results suggest that treatment with 2'3' cGAMP induces autophagic signaling in a STING-dependent manner; however, making this conclusion requires evidence of autophagy induction through inhibitor studies. To confirm autophagy induction, we treated cells with chloroquine, a lysosomotropic agent which inhibits autophagy by blocking endosomal acidification, thereby preventing amphisome formation and Atg8-II turnover[52]. Exposing wild type cells pretreated with chloroquine to 2'3' cGAMP for three hours resulted in increased levels of Atg8-II relative to Atg8-I, suggesting that 2'3' cGAMP treatment indeed induces the autophagic pathway (Fig. 6B, Fig. S6B). In cells pretreated with chloroquine, STING levels did not markedly increase after exposure to 2'3' cGAMP (Fig. S6B). We next examined whether 2'3' cGAMP induces Atg8+ puncta formation by treating wild type and *STING*$^{-}$ cells with 2'3' cGAMP for three hours, and observing mCherry foci by microscopy (Fig. 6C-F). Quantifying images revealed that Atg8+ puncta accumulate after 2'3' cGAMP treatment in wild type, but not *STING*$^{-}$ cells (Fig. 6G). Overall, these results suggest that *M. brevicollis* responds to 2'3' cGAMP through STING-dependent induction of the autophagy pathway.

Discussion

Investigating choanoflagellate immune responses has the potential to inform the ancestry of animal immune pathways. In this study, we screened bacteria to identify a choanoflagellate pathogen, and determined that *M. brevicollis* is killed by exposure to *P. aeruginosa* bacteria and selectively avoids ingesting them. We found that STING, a crucial component of animal innate responses to cytosolic DNA, is upregulated in *M. brevicollis* after exposure to *P. aeruginosa* or the STING ligand 2'3' cGAMP. Developing transgenic and genetic tools for *M. brevicollis* revealed that, similar to mammalian STING, *M. brevicollis* STING localizes to perinuclear endoplasmic reticulum regions. In addition, STING mediates responses to *P. aeruginosa* bacteria, and is required for inducing transcriptional changes and autophagic signaling in response to 2'3' cGAMP. These data reveal that STING plays conserved roles in choanoflagellate immune responses, and provide insight into the evolution of STING signaling on the animal stem lineage.

Future characterization of *M. brevicollis* STING will further elucidate its physiological roles in choanoflagellates. For example, while our results demonstrate that *M. brevicollis* STING responds to exogenous 2'3' cGAMP, the endogenous mechanisms by which STING is activated in *M. brevicollis* remain to be determined. *M. brevicollis* has a putative cGAS homolog, suggesting that STING may respond to an endogenously produced cyclic dinucleotide similar to 2'3' cGAMP, though further studies are required to determine whether this enzyme synthesizes cyclic dinucleotides, and identify ligand(s), such as dsDNA, that bind *M. brevicollis* cGAS. Although cGAS and STING are rare among sequenced choanoflagellate species, both species with STING homologs, *M. brevicollis* and *S. macrocollata*, also harbor a cGAS homolog (Fig. S1A), raising the possibility that a cGAS-STING pathway is present in some choanoflagellates

Our results suggest that *M. brevicollis* has distinct responses to 2'3' cGAMP versus 3'3'-linked cyclic dinucleotides produced by bacteria (Fig. 3C,D, Fig. S3). In contrast to 2'3' cGAMP, bacterial cyclic dinucleotides (3'3' cGAMP, c-di-AMP, c-di-GMP) do not induce cell death in *M. brevicollis*. However, 3'3' cGAMP induces a robust transcriptional response in *M. brevicollis* (Fig. S3B,C), indicating that STING, or a different cyclic dinucleotide receptor[54], responds to these bacterial molecules. One hypothesis is that *M. brevicollis* STING, similar to animal STING proteins[14], may have different binding affinities for 2'3' and 3'3'-linked cyclic dinucleotides. It is also possible that bacterial cyclic dinucleotides activate additional pathways that influence survival in *M. brevicollis*. As bacterivores, choanoflagellates likely benefit from a fine-tuned response to bacterial cyclic dinucleotides that enables them to interpret higher and lower concentrations in their environment. Elucidating mechanisms of STING activation in *M. brevicollis* could also lend understanding to how STING proteins in animals evolved to respond to both bacterially-produced and endogenous cyclic dinucleotides.

How STING initiates downstream responses in choanoflagellates is another area for further inquiry. Much of what is known about STING signaling comes from mammals and involves immune genes that are restricted to vertebrates. However, two pathways downstream of STING activation that are also present in invertebrates, and as such are proposed 'ancestral' functions of STING, are autophagy and NF-kB signaling. Here, we observed that exposure to 2'3' cGAMP induces autophagy in *M. brevicollis,* and that STING is required for autophagic pathway induction (Fig. 6). These data indicate that the role of STING in regulating autophagy predates animal origins. STING acts upstream of NF-kB in response to bacterial and viral challenge in insects[28,48–50], and 2'3' cGAMP-treatment induces the expression of NF-kB in *N. vectensis*[55]. While NF-kB homologs are detected in several choanoflagellate species, the role of NF-kB in choanoflagellates has not been studied, and neither *M. brevicollis* nor *S. macrocollata*, the two choanoflagellate species with STING, possess a NF-kB homolog[3]. This does not negate the hypothesis that STING signaling led to NF-kB activation in the Urmetazoan, but strongly suggests that additional pathways exist downstream of STING activation in choanoflagellates, and potentially in animals.

Choanoflagellates forage on diverse environmental bacteria for sustenance, yet how they recognize and respond to pathogens is a mystery. Our finding that *P. aeruginosa* has pathogenic effects on *M. brevicollis* (Fig. 1) provides a much needed framework for uncovering mechanisms of antibacterial immunity in choanoflagellates. Moreover, the discovery that *M. brevicollis* specifically avoids ingesting *P. aeruginosa* will facilitate investigating how choanoflagellates sense bacterial prey for phagocytosis. Identifying specific *P. aeruginosa* virulence factors will provide additional tools for investigating choanoflagellate pathogen responses. While profiling the host transcriptional response to *P. aeruginosa* has already allowed us to identify choanoflagellate genes that may be involved in recognizing (C-type lectins) and combating (polysaccharide lysases, antimicrobial peptides) bacteria, hundreds of uncharacterized and choanoflagellate-specific genes are also differentially expressed in response *P. aeruginosa*, and further study of these genes has the potential to reveal new mechanisms of eukaryotic immunity.

With the establishment of molecular genetic techniques in choanoflagellates -- first for *S. rosetta*[48,50], and here for *M. brevicollis* -- we now have the opportunity to explore the functions of candidate immune genes. Identifying additional choanoflagellate pathogens, particularly viral pathogens, will also be key to delineating immune response pathways. Finally, as choanoflagellates are at least as genetically diverse as animals[3], expanding studies of immune responses to diverse choanoflagellate species will be essential for reconstructing the evolution of immune pathways in animals.

Acknowledgements

We thank Bill Jackson, Tera Levin, Shally Margolis, Russell Vance, and Nan Yan for helpful advice and/or comments on the manuscript, and David Greenberg, David Hendrixson, Andrew Koh, and Kim Orth for bacterial strains. We thank Neal Alto for use of the widefield microscope, Monika Sigg for use of a reporter construct, and Mya Breitbart for sea water samples. We are grateful for David Booth's invaluable advice on developing transfection and gene editing protocols.

This work was funded by a Pew Innovation Fund award (JKP and NK), a HHMI Hanna Gray Fellows award (AW), a HHMI Faculty Scholar award (JKP), a Burroughs Wellcome Fund Investigators in the Pathogenesis of Infectious Diseases (JKP), and HHMI Investigator award (NK). We acknowledge the assistance of the UT Southwestern Live Cell Imaging Facility, a Shared Resource of the Harold C. Simmons Cancer Center, supported in part by an NCI Cancer Center Support Grant, 1P30 CA142543-01.

Methods

Culturing *M. brevicollis*

All strains of *M. brevicollis* were co-cultured with *Flavobacterium sp.* bacteria[4] (American Type Culture Collection [ATCC], Manassas, VA; Cat. No. PRA-258) in a seawater based media enriched with glycerol, yeast extract, peptone and cereal grass (details in Media Recipes). Cells were grown either at room temperature, or at 16ºC in a wine cooler (Koldfront).

Bacterial effects on *M. brevicollis*

Isolating environmental bacteria

Environmental bacterial species were isolated from water samples from Woods Hole, MA, St. Petersburg, FL, and Dallas, TX. Water samples were streaked onto Sea Water Complete media or LB plates, and grown at 30º C or 37º C. After isolating individual colonies, partial 16S sequencing using 16S universal primers (27F: 5′-AGAGTTTGATCCTGGCTCAG-3′, 1492R: 5′-TACGGYTACCTTGTTACGACTT-3′) was used to determine the identity of the bacterial isolates.

Screening for pathogenic effects

M. brevicollis was grown for 30 h, and feeding bacteria were reduced through one round of centrifugation and resuspension in artificial seawater (ASW). Cells were counted on a hemocytometer and diluted to $5x10^6$ cells/mL in High Nutrient Medium, and plated into 24-well plates.

For each bacterium, a single colony was inoculated into LB and grown shaking overnight at either 30º C (environmental isolates) or 37º C (mouse isolates). Bacterial cells were pelleted by centrifugation for 5 minutes at 4000 x *g,* and resuspended in artificial seawater (ASW) to an OD~1.

Each bacterial species was added to *M. brevicollis* culture at two concentrations (10mL/mL and 50 mL/mL) in duplicate. *M. brevicollis* was then monitored at regular intervals for changes in behavior and growth.

Growth curves in the presence of bacteria

All bacteria were grown shaking at 30º C in Sea Water Complete media or LB (to optical density of 0.8). For each bacterial strain, CFU plating was used to estimate the number of bacterial cells/ mL under these growth conditions. To prepare bacterial conditioned media, bacterial cells were pelleted by centrifugation for 10 minutes at 4000 x *g,* and supernatant was passed through a 0.22mm sterilizing filter.

M. brevicollis was grown for 30 h, and bacteria were washed away through two consecutive rounds of centrifugation and resuspension in artificial seawater (ASW). Cells were counted on a hemocytometer and diluted to $1.0x10^6$ cells/mL (growth curves with live bacteria) or $1.5x10^5$ cells/mL (growth curves with conditioned medium) in High Nutrient Medium. To test the effects of live bacteria, $1.5x10^6$ bacterial cells were added per 1 mL of *M. brevicollis* culture. To test the effects of bacterial conditioned media, 50 ml of bacterial conditioned media was added per 1 mL of *M. brevicollis* culture. For each growth curve biological replicate, cells were plated into 24-well plates, and two wells were counted per time point as technical replicates. At least three biological replicates are represented in each graph.

Bacterial internalization

Fluorescent *E. coli* and *P. aeruginosa* were grown shaking at 30º C in LB to an optical density of OD_{600}=0.8. Fluorescent *C. jejuni* was grown from freezer stocks in microaerobic conditions on Mueller-Hinton agar. For each bacterial strain, CFU plating was used to estimate the number of bacterial cells/ mL under these growth conditions.

M. brevicollis was grown for 30 h, and bacteria were washed away with one round of centrifugation and resuspension in artificial seawater (ASW). Cells were counted and diluted to $1.5x10^5$ cells/mL in ASW. $7.5x10^6$ bacterial cells were added to 5 mL *M. brevicollis* culture in a 50mL conical, and co-incubated at room temperature with gentle mixing at regular intervals. To quantify bead internalization, *M. brevicollis* was co-incubated with bacteria for 1 hour (as described above), at which point ~$1x10^{10}$ beads (0.2mm diameter, resuspended in 1% BSA to prevent clumping) were added to the conical for an additional 30 minutes.

Prior to imaging, 200mL aliquots were transferred to 8-well glass bottom chambers (Ibidi Cat. No 80827). Live imaging was performed on a Zeiss Axio Observer widefield microscope using a 63x objective. Images were processed and analyzed using Fiji[56].

P. aeruginosa deletion mutants

P. aeruginosa deletion strains were acquired from the Seattle PAO1 transposon mutant library (NIH P30 DK089507). The effects of both live bacteria and bacterial conditioned medium were tested for all acquired strains at a range of PFU/mL (live bacteria) or percent volume (conditioned medium).

Immune agonist dose-response curves

M. brevicollis was grown to late-log phase, and feeding bacteria were reduced through one round of centrifugation and resuspension in artificial seawater (ASW). Cells were counted on a hemocytometer and diluted to $1.0x10^6$ cells/mL (growth curves with live bacteria) in High Nutrient Medium, and aliquoted into 96-well (100µL/well) or 24-well (1mL/well) plates. Immune agonists were added at indicated concentrations in technical duplicate, and cells were counted again after 24 hours. % survival is a calculation of: [mean experimental (cells/mL) / mean control (cells/mL)]. Each dose-response curve is representative of at least three biological replicates.

RNA-seq

Growth of choanoflagellate cultures

After thawing new cultures, growth curves were conducted to determine the seeding density and time required to harvest cells at late-log phase growth. To grow large numbers of cells for RNA-seq, cells were seeded one to two days prior to the experiment in either 3-layer flasks (Falcon; Corning, Oneonta, NY, USA; Cat. No. 14-826-95) or 75 cm^2 flasks (Falcon; Corning, Oneonta, NY, USA; Cat. No. 13-680-65), and grown at room temperature. Bacteria were washed away from choanoflagellate cells through two rounds of centrifugation and resuspension in artificial seawater (ASW). To count the cell density, cells were diluted 100-fold in 200 µl of ASW, and fixed with 1 µL of 16% paraformaldehyde. Cells were counted on a hemocytometer, and the remaining cells were diluted to a final concentration of $4×10^6$ choanoflagellate cells/mL. The resuspended cells were divided into 2.5 mL aliquots and plated in 6-well plates prior to treatment. After treatment, cells were transferred to a 15 mL conical and pelleted by centrifugation at 2400 x *g* for 5 min, flash frozen with liquid nitrogen, and stored at -80°C.

RNA isolation

Total RNA was isolated from cell pellets with the RNAqueous kit (Ambion, Thermo Fisher Scientific). Double the amount of lysis buffer was used to increase RNA yield and decrease degradation, and RNA was eluted in minimal volumes in each of the two elution steps (40 µL and 15 µL). RNA was precipitated in LiCl to remove contaminating genomic DNA. Total RNA concentration and quality was evaluated using the Agilent Bioanalyzer 2100 system and RNA Nano Chip kit (Cat No. 5067-1511).

Library preparation, sequencing, and analysis

Libraries were prepared and sequenced by the UTSW Genomics Sequencing Core. RNA libraries were generated with the Illumina TruSeq® Stranded mRNA Library prep kit (Cat No. 20020594), using a starting total RNA input of 2-3 µg. To remove contaminating bacterial RNA, samples were first poly-A selected using oligo-dT attached magnetic beads. Following purification, the mRNA was fragmented at 94ºC for 4 minutes, and cleaved RNA fragments were synthesized into cDNA. After an end repair step, UMI adapters (synthesized by IDT) were ligated to the cDNA, and the products were twice purified using AMPure XP beads before amplification. Library quantity was measured using the Quant-iT™ PicoGreen dsDNA Assay kit by Invitrogen (Cat No. P7589) and a PerkinElmer Victor X3, 2030 Multilabel Reader. Library quality was verified on an Agilent 2100 Bioanalyzer instrument using Agilent High sensitivity DNA kit (Cat No. 5067-4626) or DNA 1000 kit (Cat No. 5067-1504). Libraries were pooled, and sequenced in different batches on either the Illumina NextSeq 550 system with SE-75 workflow, or the Illumina NovaSeq 6000 system with S4 flowcell and XP PE-100 workflow, generating 25-40 million reads per sample. Reads were checked for quality using fastqc (v0.11.2) and fastq_screen (v0.4.4), and trimmed using fastq-mcf (ea-utils, v1.1.2-806). Trimmed fastq files were mapped to the *Monosiga brevicollis* reference genome (NCBI:txid81824) using TopHat[57] (v2.0.12). Duplicates were marked using picard-tools (v2.10.10). Read counts were generated using featureCounts[58], and differential expression analysis was performed using edgeR[59]. Statistical cutoffs of FDR≤10^{-4} were used to identify significant differentially expressed genes. GO enrichment analysis of differentially expressed genes was performed using DAVID (https://david.ncifcrf.gov/).

Immunoblotting

M. brevicollis was harvested by centrifugation at 5,000 x *g* for 5 min at 4°C, and resuspended in 100 µL lysis buffer (50mM Tris, pH 7.4, 150 mM NaCl, 1 mM EDTA, 1 mM ethyleneglycoltetraacetic acid [EGTA], 0.5% sodium deoxycholate, 1% NP-40) containing protease inhibitor cocktail (Roche) for 10 min at 4°C. The crude lysate was clarified by centrifugation at 10,000 x *g* for 10 min at 4°C, and denatured in Laemmli buffer before SDS-PAGE. Proteins were transferred to an Immobilon-P PVDF membrane (Millipore), and blocked for two hours in PBST (1x PBS containing 5% nonfat dry milk and 0.05% Tween-20). Membranes were incubated with primary antibodies diluted in PBST overnight at 4°C and washed extensively in PBST. Membranes were incubated with secondary antibodies for 1 hour at room temperature, washed extensively in PBST, and developed using Immobilon Western Chemiluminescent HRP Substrate (Millipore Sigma).

STING antibody production

The anti-mbreSTING antibody was generated by Pacific Immunology. Rabbits were immunized with a KLH-conjugated peptide corresponding to residues 320-338 of

M. brevicollis protein EDQ90889.1 (Cys-KNRSEVLKKMRAEDQYAMP), and serum was affinity purified against the peptide to reduce cross-reactivity and validated using immunoblotting.

Immunofluorescence Staining and Imaging

Depending on the cell density of the starting culture, between 0.2-1 mL of cells were concentrated by centrifugation for 5 min at 2500 × *g*. The cells were resuspended in 200 µl of artificial seawater and applied to poly-L-lysine–coated coverslips (Corning Life Sciences; Cat. No.354085) placed at the bottom of each well of a 24-well cell culture dish. After the cells were allowed to settle on the coverslip for 30 min, 150 µl of the cell solution was gently removed from the side of the dish. All of the subsequent washes and incubations during the staining procedure were performed by adding and removing 200 µl of the indicated buffer.

Cells were fixed in two stages. First, 200 µl cold 6% acetone diluted in 4X PBS was added for 5 min at room temperature. Next, 200 µl cold 8% paraformaldehyde diluted in 4X PBS was added (yielding a final concentration of 4% paraformaldehyde), and the fixative mixture was incubated for 15 min at room temperature. After fixation, the coverslip was gently washed three times with 200 µl 4X PBS.

Cells were permeabilized by incubating in permeabilization buffer (4X PBS; 3% [wt/vol] bovine serum albumin (BSA)-fraction V; 0.2% [vol/vol] Triton X-100) for 30 min. After removing permeabilization buffer, the coverslip was incubated in primary antibody for 1 hour at room temperature, and then washed three times in 4X PBS. The coverslip was then incubated with secondary antibody for 1 hour at room temperature, and then washed twice in 4X PBS. The coverslip was next incubated in 4 U/ml Phalloidin (Thermo Fisher Scientific) for 30 min at room temperature, washed once in 4X PBS. Lastly, the coverslip was incubated in 10 µg/ml Hoechst 33342 (Thermo Fisher Scientific) for 5 min at room temperature, and then washed once with 4X PBS.

To prepare a slide for mounting, 10 µl of Pro-Long Gold (Thermo Fisher Scientific) was added to a slide. The coverslip was gently removed from the well with forceps, excess buffer was blotted from the side with a piece of filter paper, and the coverslip was gently placed on the drop of Pro-Long diamond. The mounting media cured overnight before visualization.

Images were acquired on either: (1) a Zeiss LSM 880 Airyscan confocal microscope with a 63x objective by frame scanning in the superresolution mode (images processed using the automated Airyscan algorithm (Zeiss)), or (2) a Nikon CSU-W1 SoRa spinning disk confocal microscope with a 60x objective in SR mode (images processed using Imaris).

Live-Cell Imaging

599 Cells transfected with fluorescent reporter plasmid were prepared for microscopy
600 by transferring 200 µl of cells to a glass-bottom dish or glass-bottom 8-well chamber
601 (Ibidi). Confocal microscopy was performed on a Zeiss Axio Observer LSM 880 with an
602 Fast Airyscan detector and a 63x/NA1.40 Plan-Apochromatic oil immersion objective
603 (Carl Zeiss AG, Oberkochen, Germany). Confocal stacks were acquired by frame
604 scanning in superresolution mode, and images were processed using the automated
605 Airyscan algorithm (Zeiss).
606
607 Transfection of *M. brevicollis*
608 ***Cell Culture.*** One day prior to transfection, 60 ml of High Nutrient Medium was
609 inoculated with *M. brevicollis* to a final concentration of 10000 cells/ml. The culture was
610 split in two, and grown in two 75 cm^2 flasks at room temperature, approximately 22°C
611 (Falcon; Corning, Oneonta, NY, USA; Cat. No. 13-680-65).
612 ***Cell Washing.*** After 24 hours of growth, bacteria were washed away from *M.*
613 *brevicollis* cells through three consecutive rounds of centrifugation and resuspension in
614 artificial seawater (ASW). The culture flasks were combined and vigorously shaken for
615 30 s, and then transferred to 50-ml conical tubes and spun for 5 min at 2000 × *g* and
616 22°C. The supernatant was removed with a serological pipette, and residual media were
617 removed with a fine-tip transfer pipette. The cell pellets were resuspended in a single
618 conical tube in a total volume of 50 ml of ASW, vigorously shaken for 30 s, and then
619 centrifuged for 5 min at 2050 × *g*. The supernatant was removed as before. In a final
620 washing step, the cell pellet was resuspended in 50 mL ASW, shaken vigorously, and
621 centrifuged for 5 min at 2100 × *g*. After the supernatant was removed, the cells were
622 resuspended in a total volume of 400 µl of ASW. To count the cell density, cells were
623 diluted 100-fold in 200 µl of ASW, and fixed with 1 µl of 16% paraformaldehyde. Cells
624 were counted on a hemocytometer, and the remaining cells were diluted to a final
625 concentration of 5×10^7 choanoflagellate cells/ml. The resuspended cells were divided
626 into 100-µl aliquots with 5×10^6 cells per aliquot to immediately prime cells in the next
627 step.
628 ***Cell Priming.*** Each aliquot of *M. brevicollis* cells was incubated in priming buffer (40
629 mM HEPES-KOH, pH 7.5; 55 mM lithium citrate; 50 mM L-cysteine; 10% [wt/vol] PEG
630 8000; and 2 µM papain) to remove the extracellular material coating the cell. The 100-µl
631 aliquots, which contained 5×10^6 cells, were centrifuged for 5 min at 1700 × *g*. The
632 supernatant was removed, and cells were resuspended in 100 µl of priming buffer and
633 then incubated for 35 min at room temperature. Priming was quenched by adding 4 µl of
634 50-mg/ml bovine serum albumin-fraction V (Thermo Fisher Scientific, Waltham, MA;
635 Cat. No. BP1600-100) and then centrifuged for 5 min at 1250 ×*g* and 22°C with the
636 centrifuge brake set to a “soft” setting. The supernatant was removed with a fine-tip
637 micropipette, and the cells were resuspended in 25 µl of SG Buffer (Lonza).

Nucleofection. Each transfection reaction was prepared by adding 2 µl of "primed" cells resuspended in SG buffer (Lonza) to a mixture of: 16 µl of SG buffer, 2 µl of 20 µg/µl pUC19, 1 µl of 250 mM ATP (pH 7.5), 1 µl of 100 mg/ml sodium heparin, and ≤7 µl of reporter DNA (volume is dependent on the number of constructs transfected). Each transfection reaction was transferred to one well in 16-well nucleofection strip (Lonza; Cat. No. V4XC-2032). The nucleofection strip was placed in the X-unit (Lonza; Cat. No. AAF-1002F) connected to a Nucleofector 4D core unit (Lonza; Cat. No. AAF-1002B), and the EO100 pulse was applied to each well.

Recovery. 100 µl of cold recovery buffer (10 mM HEPES-KOH, pH 7.5; 0.9 M sorbitol; 8% [wt/vol] PEG 8000) was added to the cells immediately after pulsation. After 5 minutes, the whole volume of the transfection reaction plus the recovery buffer was transferred to 2 ml of Low Nutrient Medium in a 12-well plate. The cells were grown for 24–48 hours before being assayed for luminescence or fluorescence.

Puromycin Selection. To generate stably transfected *M. brevicollis* cell lines, puromycin was added to cells 24 hours after transfection at a final concentration of 300 µg/mL. Cells were monitored over the course of 7-21 days, and fresh High Nutrient Media + 300 µg/mL puromycin was added to the cells as needed.

Genome editing

For a more detailed description of gRNA and repair oligonucleotide design, refer to Booth et al. 2018[48].

Design and preparation of gRNAs First, crRNAs were designed by using the extended recognition motif 5'-HNNGRSGGH-3' (in which the PAM is underlined, N stands for any base, R stands for purine, S stands for G or C, and H stands for any base except G) to search for targets in cDNA sequences[60]. Next, we confirmed that the RNA sequence did not span exon-exon junctions by aligning the sequence to genomic DNA.

Functional gRNAs were prepared by annealing synthetic crRNA with a synthetic tracrRNA[50]. To prepare a functional gRNA complex from synthetic RNAs, crRNA and tracrRNA (Integrated DNA Technologies [IDT], Coralville, IA, USA) were resuspended to a final concentration of 200 µM in duplex buffer (30 mM HEPES-KOH, pH 7.5; 100 mM potassium acetate; IDT, Cat. No. 11-0103-01). Equal volumes of crRNA and tracrRNA stocks were mixed together, incubated at 95°C for 5 min in an aluminum block, and then the entire aluminum block was placed at room temp to slowly cool the RNA to 25°C. The RNA was stored at -20°C

673 ***Design and preparation of repair oligonucleotides*** Repair oligonucleotides for
674 generating knockouts were designed by copying the sequence 50 bases upstream and
675 downstream of the SpCas9 cleavage site. A knockout sequence
676 (5'TTTATTTAATTAAATAAA-3') was inserted at the cleavage site[50].
677 Dried oligonucleotides (IDT) were resuspended to a concentration of 250 µM in a
678 buffer of 10 mM HEPES-KOH, pH 7.5, incubated at 55°C for 1 hour, and mixed well by
679 pipetting up and down. The oligonucleotides were stored at -20°C.
680 ***Delivery of gene editing cargoes with nucleofection***
681 The method for delivering *Sp*Cas9 RNPs and DNA repair templates into *M.*
682 *brevicollis* is as follows:
683 ***Cell Culture.*** One day prior to transfection, 60 ml of High Nutrient Medium was
684 inoculated to a final concentration of *M. brevicollis* at 10000 cells/ml. The culture was
685 split in two, and grown in two 75 cm^2 flasks at room temperature, approximately 22°C
686 (Falcon; Corning, Oneonta, NY, USA; Cat. No. 13-680-65).
687 ***Assembly of Cas9/gRNA RNP.*** Before starting transfections, the *Sp*Cas9 RNP was
688 assembled. For one reaction, 2 µl of 20 µM *Sp*Cas9 (NEB, Cat. No. M0646M) was
689 placed in the bottom of a 0.25 ml PCR tube, and then 2 µl of 100 µM gRNA was slowly
690 pipetted up and down with *Sp*Cas9 to gently mix the solutions. The mixed solution was
691 incubated at room temperature for 1 hour, and then placed on ice.
692 ***Thaw DNA oligonucleotides.*** Before using oligonucleotides in nucleofections, the
693 oligonucleotides were incubated at 55°C for 1 hour.
694 ***Cell Washing.*** After 24 hours of growth, bacteria were washed away from *M.*
695 *brevicollis* cells through three consecutive rounds of centrifugation and resuspension in
696 artificial seawater (ASW). The culture flasks were combined and vigorously shaken for
697 30 s, and then transferred to 50-ml conical tubes and spun for 5 min at 2000 × *g* and
698 22°C. The supernatant was removed with a serological pipette, and residual media were
699 removed with a fine-tip transfer pipette. The cell pellets were resuspended in a single
700 conical tube in a total volume of 50 ml of ASW, vigorously shaken for 30 s, and then
701 centrifuged for 5 min at 2050 × *g*. The supernatant was removed as before. In a final
702 washing step, the cell pellet was resuspended in 50 mL ASW, shaken vigorously, and
703 centrifuged for 5 min at 2100 × *g*. After the supernatant was removed, the cells were
704 resuspended in a total volume of 400 µl of ASW. To count the cell density, cells were
705 diluted 100-fold in 200 µl of ASW, and fixed with 1 µl of 16% paraformaldehyde. Cells
706 were counted on a hemocytometer, and the remaining cells were diluted to a final
707 concentration of 5 × 10^7 choanoflagellate cells/ml. The resuspended cells were divided
708 into 100-µl aliquots with 5 × 10^6 cells per aliquot to immediately prime cells in the next
709 step.
710 ***Cell Priming.*** Each aliquot of *M. brevicollis* cells was incubated in priming buffer (40
711 mM HEPES-KOH, pH 7.5; 50 mM lithium citrate; 50 mM L-cysteine; 15% [wt/vol] PEG
712 8000; and 2 µM papain) to remove the extracellular material coating the cell. The 100-µl

aliquots, which contained 5 × 10^6 cells, were centrifuged for 5 min at 1700 × *g* and at room temperature. The supernatant was removed, and cells were resuspended in 100 µl of priming buffer and then incubated for 35 min. Priming was quenched by adding 10 µl of 50-mg/ml bovine serum albumin-fraction V (Thermo Fisher Scientific, Waltham, MA; Cat. No. BP1600-100). Cells were then centrifuged for 5 min at 1250 ×*g* and 22°C with the centrifuge brake set to a "soft" setting. The supernatant was removed with a fine-tip micropipette, and the cells were resuspended in 25 µl of SG Buffer (Lonza).

Nucleofection. Each nucleofection reaction was prepared by adding 16 µl of cold SG Buffer to 4 µl of the *Sp*Cas9 RNP that was assembled as described above. For reactions that used two different guide RNAs, each gRNA was assembled with *Sp*Cas9 separately and 4 µl of each RNP solution were combined at this step. 2 µl of the repair oligonucleotide template was added to the *Sp*Cas9 RNP diluted in SG buffer. Finally, 2 µl of primed cells were added to the solution with Cas9 RNP and the repair template. The nucleofection reaction was placed in one well of a 16-well nucleofection strip (Lonza; Cat. No. V4XC-2032). The nucleofection strip was placed in the X-unit (Lonza; Cat. No. AAF-1002F) connected to a Nucleofector 4D core unit (Lonza; Cat. No. AAF-1002B), and the EO100 pulse was applied to each well.

Recovery. 100 µl of cold recovery buffer (10 mM HEPES-KOH, pH 7.5; 0.9 M sorbitol; 8% [wt/vol] PEG 8000) was added to the cells immediately after pulsation. After 5 minutes, the whole volume of the transfection reaction plus the recovery buffer was transferred to 1 ml of High Nutrient Medium in a 12-well plate.

Cycloheximide Selection in M. brevicollis. One day after transfection, 10 µl of 10 µg/ml cycloheximide was added per 1 mL culture of transfected cells. The cells were incubated with cycloheximide for 5 days prior to clonal isolation and genotyping.

Genotyping. Cells were harvested for genotyping by spinning 0.5ml of cells at 4000*g* and 22°C for 5 min. The supernatant was removed and DNA was isolated either by Base-Tris extraction [in which the cell pellet was resuspended in 20uL base solution (25mM NaOH, 2mM EDTA), boiled at 100°C for 20 min, cooled at 4°C for 5 min, and neutralized with 20uL Tris solution (40mM Tris-HCl, pH 7.5)], or by DNAzol Direct [in which the cell pellet was resuspended in 50uL and incubated at room temperature for 30 min (Molecular Research Center, Inc. [MRC, Inc.], Cincinnati, OH; Cat. No. DN131)]. 3 µl of the DNA solution was added to a 25 µl PCR reaction (DreamTaq Green PCR Master Mix, Thermo Fisher Scientific Cat No K1082) and amplified with 34 rounds of thermal cycling.

Data Availability

Raw sequencing reads and normalized gene counts have been deposited at the NCBI GEO under accession GSE174340.

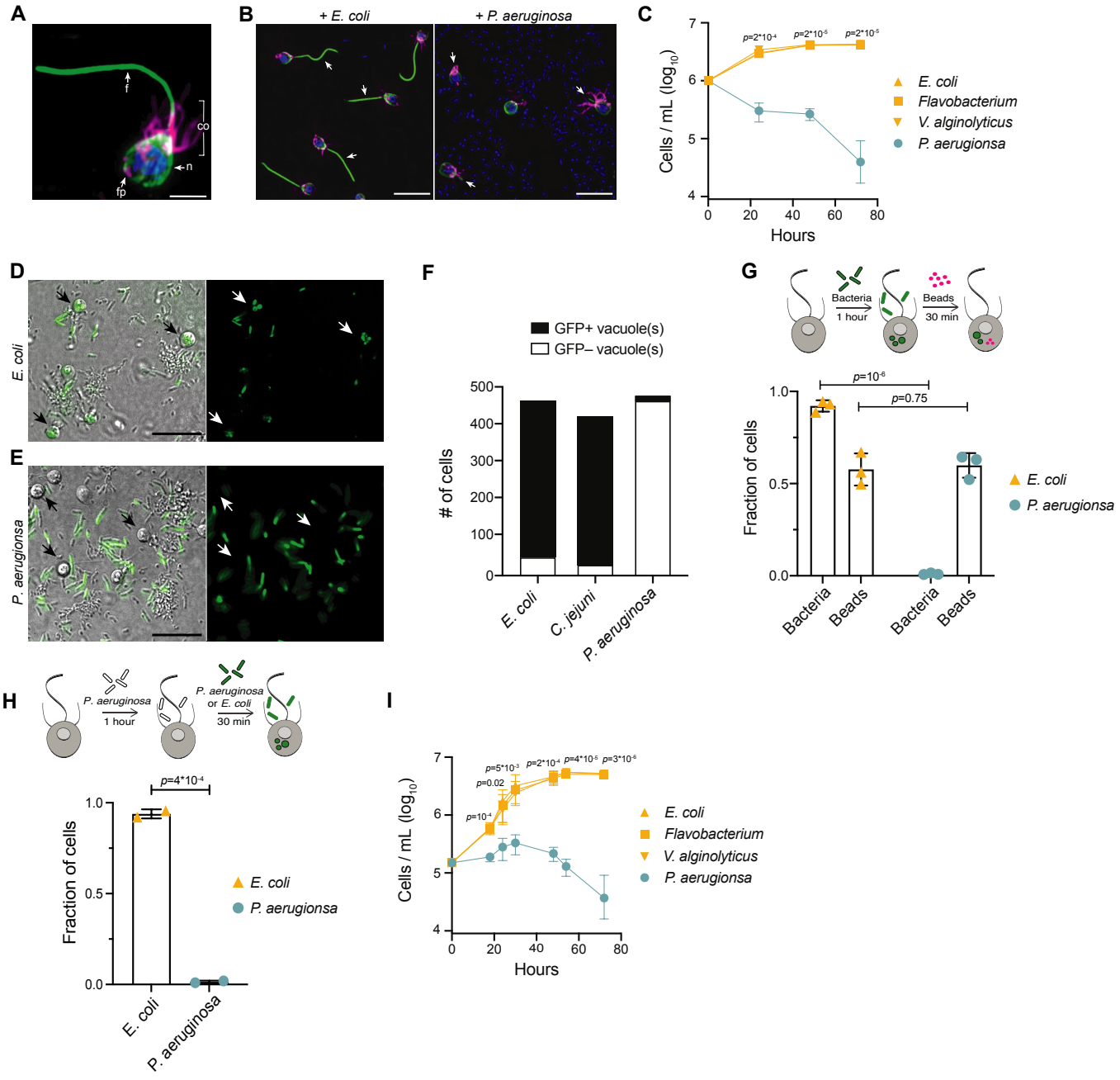

Figure 1. *P. aeruginosa* has pathogenic effects on *M. brevicollis*

(A) Immunofluorescence illuminates the diagnostic cellular architecture of *M. brevicollis*, including an apical flagellum (f) made of microtubules, surrounded by an actin-filled microvilli feeding collar (co). Staining for tubulin (green) also highlights cortical microtubules that run along the periphery of the cell body, and staining for F-actin (magenta) highlights basal filopodia (fp). DNA staining (blue) highlights the nucleus (n). **(B)** *M. brevicollis* exhibits truncated flagella after exposure to *P. aeruginosa. M.*

brevicollis were exposed to *E. coli* or *P. aeruginosa* for 24 hours, and then fixed and immunostained. Arrows point to flagella. Green: anti-tubulin antibody (flagella and cell body), magenta: phalloidin (collar), blue: Hoechst (bacterial and choanoflagellate nuclei). Scale bars represent 10μm. **(C)** Exposure to *P. aeruginosa*, but not other Gammaproteobacteria, results in *M. brevicollis* cell death. Bacteria were added to *M. brevicollis* culture at an MOI of 1.5 (at Hours=0), and *M. brevicollis* cell density was quantified at indicated time points. Data represent mean +/- SD for three biological replicates. Statistical analysis (multiple unpaired t-tests) was performed in GraphPad software; *p*-values shown are from comparisons between *Flavobacterium* and *P. aeruginosa.* (**D-F)** *M. brevicollis* does not ingest *P. aeruginosa* bacteria. **(D,E)** *M. brevicollis* were fed either fluorescent *E. coli* (D) or *P. aeruginosa* (E) for one hour, and then visualized by DIC (D,E, left) and green fluorescence (D, E, right). Fluorescent food vacuoles were observed in choanoflagellates fed *E. coli,* but not *P. aeruginosa.* **(F)** Cells were fed fluorescent bacteria for one hour, and then imaged by DIC and green fluorescence. Cells with ≥1 GFP+ food vacuole were scored as GFP+, and cells without any GFP+ food vacuoles were scored as GFP–. Data represent three biological replicates. **(G,H)** *M. brevicollis* selectively avoids eating *P. aeruginosa*. **(G)** Internalization of 0.2μm fluorescent beads was used to quantify phagocytic activity after exposure to *E. coli* or *P. aeruginosa* bacteria. Although cells did not phagocytose *P. aeruginosa,* cells exposed to *E. coli* and *P. aeruginosa* had similar phagocytic uptake of beads. Data represent n=600 cells from three biological replicates. Statistical analyses (multiple unpaired t-tests) were performed in GraphPad software. **(H)** Exposure to *P. aeruginosa* does not inhibit phagocytic uptake of *E. coli.* Internalization of fluorescent *E. coli* or *P. aeruginosa* bacteria was quantified after exposure to unlabeled *P. aeruginosa* (PAO1 strain). Data represent n=200 cells from two biological replicates. Statistical analysis (unpaired t-test) was performed in GraphPad software. **(I)** Secreted *P. aeruginosa* molecules are sufficient to induce *M. brevicollis* cell death. 5% (vol/vol) bacterial conditioned medium was added to *M. brevicollis* culture (at Hours=0), and *M. brevicollis* cell density was quantified at indicated time points. Data represent mean +/- SD for three biological replicates. Statistical analysis (multiple unpaired t-tests) was performed in GraphPad software, and *p*-values shown are from comparisons between *Flavobacterium* and *P. aeruginosa.*

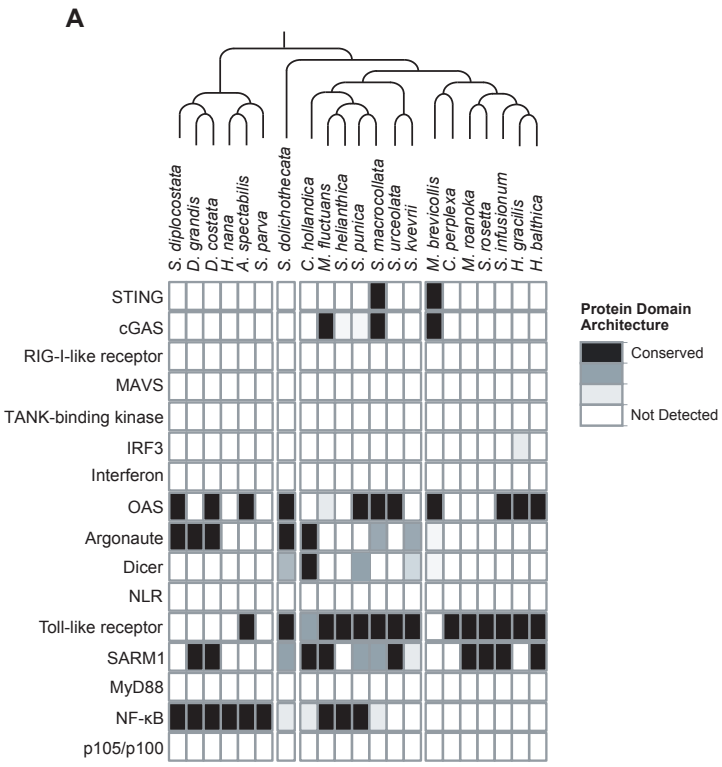

Supplemental Figure 1. Presence of animal innate immune genes in choanoflagellates (A) The transcriptomes of 21 choanoflagellate species[3] were searched for genes that play key roles in animal innate immune responses. Evidence for gene presence was based on sequence homology in a BLAST-based approach and conserved domain architectures, as described in Richter et al., 2018.

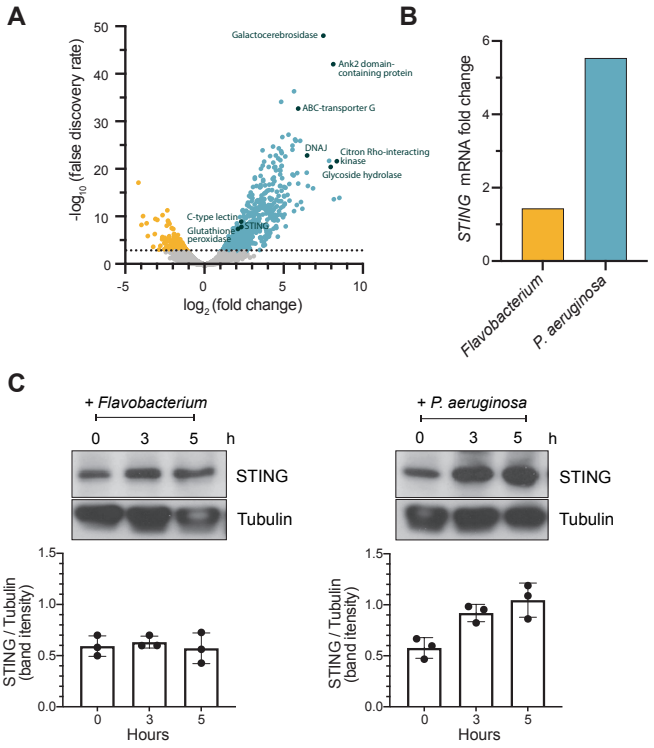

Figure 2. STING is upregulated in *M. brevicollis* after exposure to *P. aeruginosa*
(A,B) *STING* transcript levels increase in response to *P. aeruginosa.* **(A)** Volcano plot displaying genes differentially expressed between *M. brevicollis* exposed to *P. aeruginosa* PAO1 and *Flavobacterium* (control) conditioned medium for three hours. Differentially expressed genes are depicted by blue (674 upregulated genes) and yellow (232 downregulated genes) dots (fold change≥2; FDR≤1e^{-4}). Select genes that are upregulated or may function in innate immunity are labeled. RNA-seq libraries were prepared from four biological replicates. **(B)** After a three-hour treatment, *STING* mRNA levels (determined by RNA-seq) increase 1.42 fold in cells exposed to *Flavobacterium* conditioned medium and 5.54 fold in cells exposed to *P. aeruginosa* conditioned medium, compared to untreated controls. **(C)** STING protein levels increase after exposure to *P. aeruginosa*. STING levels were examined by immunoblotting at indicated timepoints after exposure to *Flavobacterium* or *P. aeruginosa* conditioned medium (5% vol/vol). Tubulin is shown as loading control, and intensity of STING protein bands were quantified relative to tubulin.

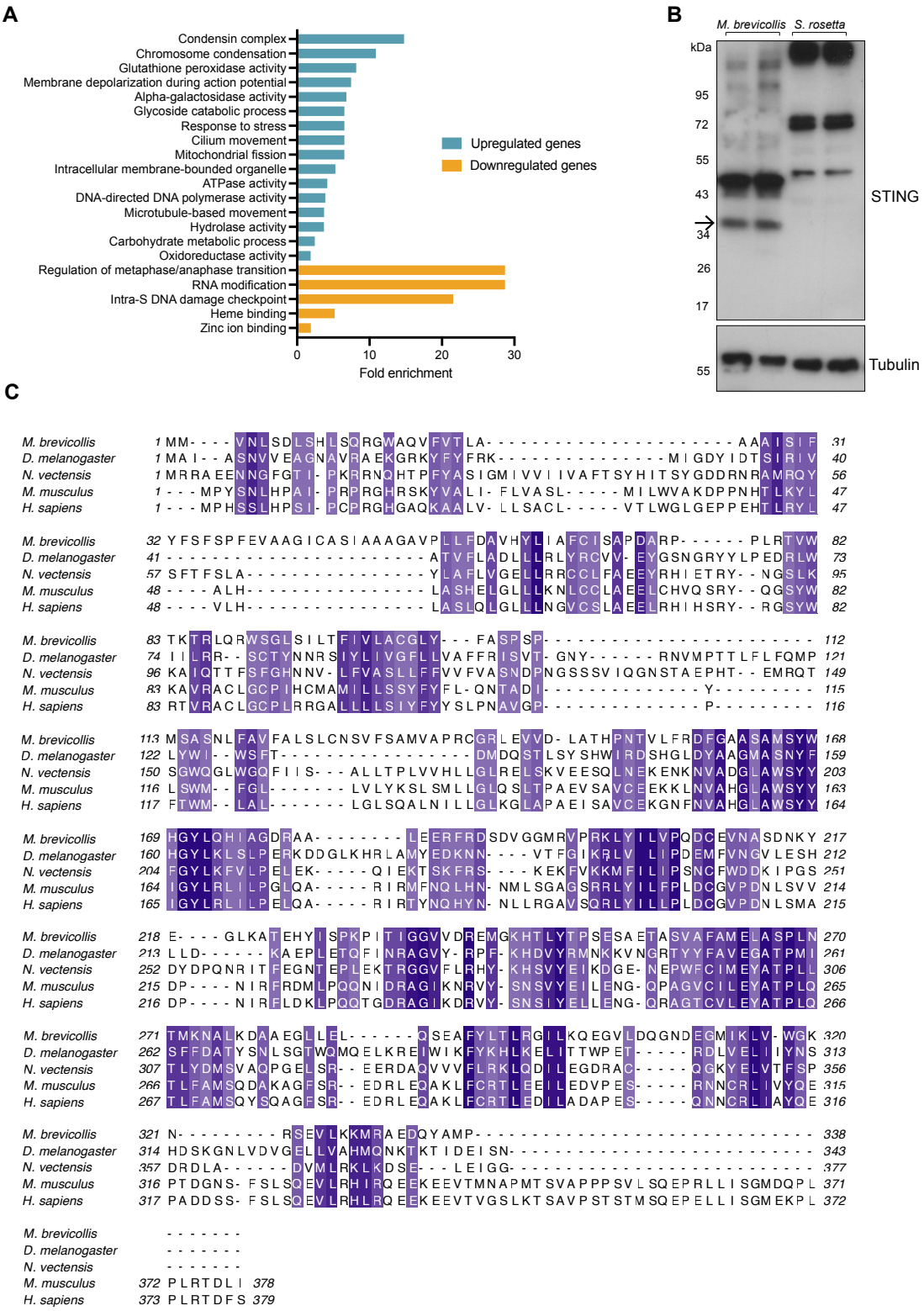

Supplemental Figure 2. *M. brevicollis* response to *P. aeruginosa,* and STING antibody validation and protein alignment. (A) Gene ontology enrichment analysis of genes identified as differentially expressed (fold change≥2; FDR≤1e^{-4}) after exposure to

P. aeruginosa. Due to lack of annotation, >40% of the differentially expressed genes were not included in the enrichment analysis. **(**B**)** To validate the *M. brevicollis* STING antibody, cell lysates from *M. brevicollis* were immunoblotted alongside cell lysates from *S. rosetta,* a closely-related choanoflagellate species that does not have a STING homolog. A band at 36kD, the predicted size of *M. brevicollis* STING, is detectable in *M. brevicollis* lysate but not *S. rosetta* lysate. Arrow indicates STING band. Non-specific bands are likely due to co-cultured feeding bacteria. Tubulin is shown as loading control. (**C)** Protein sequence alignment (generated by Clustal Omega multiple sequence alignment) of *M. brevicollis* and animal STING proteins, colored by similarity. *M. brevicollis* STING and human STING are 19.1% identical and 36.6% similar at the amino acid level.

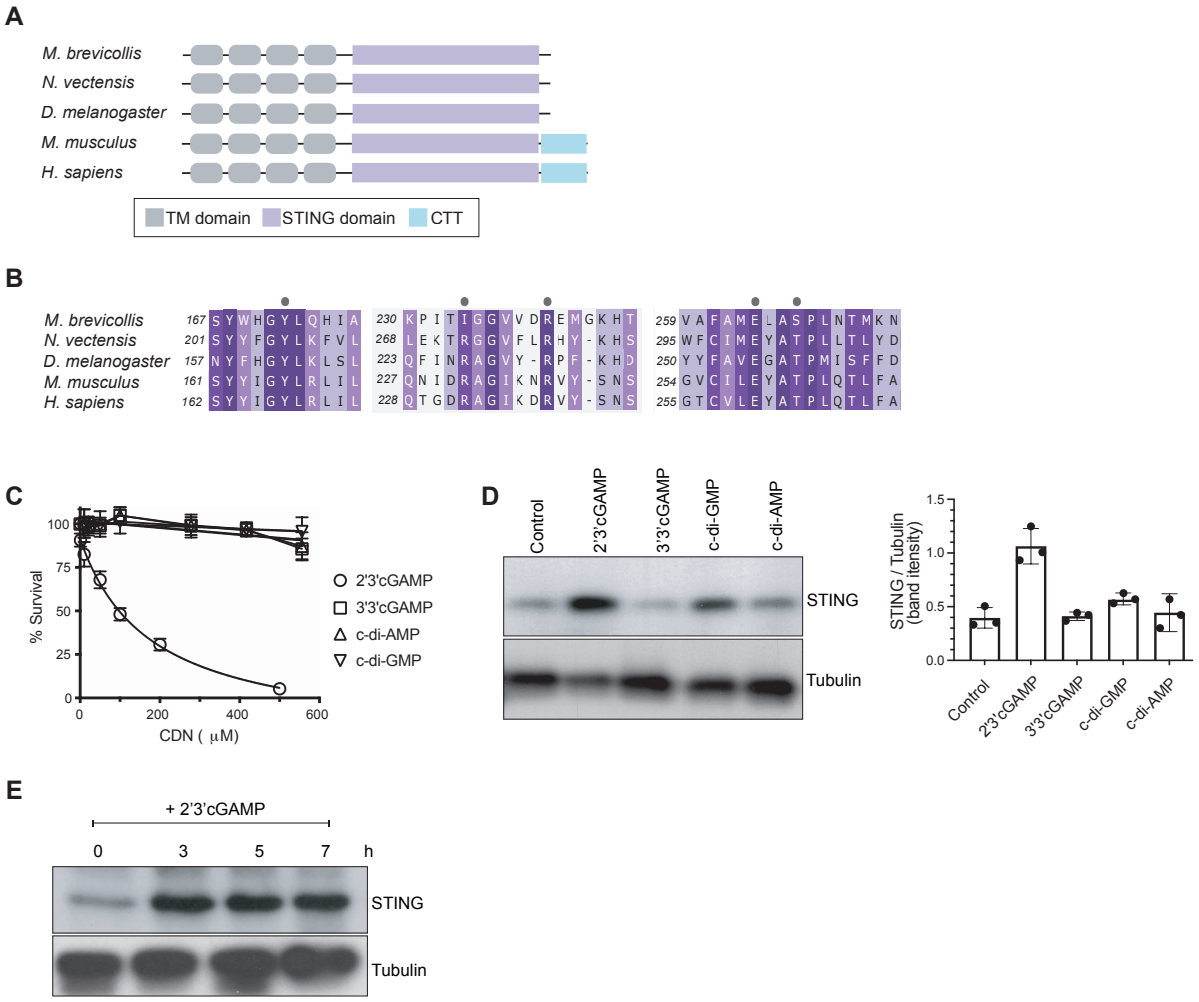

Figure 3. 2'3' cGAMP, but not bacterially-produced cyclic dinucleotides, induces elevated levels of STING

(A) Schematic of choanoflagellate (*M. brevicollis*), sea anemone (*N. vectensis*), insect (*D. melanogaster*) and mammalian (*M. musculus* and *H. sapiens*) STING proteins. Transmembrane (TM) domains are depicted in gray, STING cyclic dinucleotide binding domain (CDN) in purple, and C-terminal tail domain (CTT) in blue. **(B)** Partial protein sequence alignment (generated by Clustal Omega multiple sequence alignment) of *M. brevicollis* and animal STING proteins, colored by similarity. *M. brevicollis* STING and human STING are 19.1% identical and 36.6% similar at the amino acid level. Key cyclic dinucleotide-interacting residues from human STING structure are indicated by circles. **(C)** Dose-response curves of *M. brevicollis* exposed to cyclic dinucleotides for 24 hours reveal that treatment with 2'3'cGAMP, but not 3'3' cGAMP, c-di-AMP, or c-di-GMP, leads to *M. brevicollis* cell death in a dose-dependent manner. Data represent mean +/- SD for at least three biological replicates. **(D)** STING protein levels increase after exposure to 2'3'cGAMP, but not bacterially-produced cyclic dinucleotides. *M. brevicollis*

STING levels were examined by immunoblotting 5 hours after exposure to 2'3'cGAMP (100 μM), 3'3'cGAMP (200 μM), c-di-GMP (200 μM), or c-di-AMP (200 μM). Tubulin is shown as loading control, and intensity of STING protein bands were quantified relative to tubulin. Shown is a representative blot from three biological replicates. **(E)** STING protein levels increase and remain elevated after exposure to 100μM 2'3'cGAMP. Tubulin is shown as loading control, and data are representative of three biological replicates.

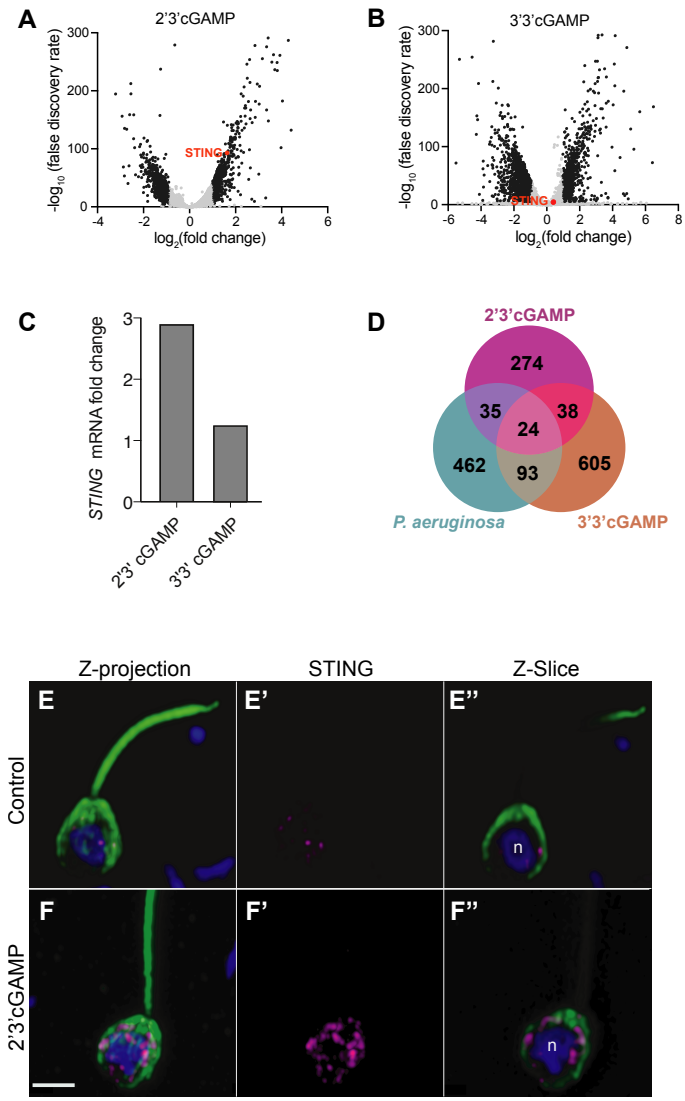

Supplemental Figure 3. *M. brevicollis* has distinct responses to 2'3' cGAMP and 3'3' cGAMP

(A,B) Volcano plots displaying RNA-seq differential expression analysis of *M. brevicollis* treated with (A) 100 μM 2'3'cGAMP or (B) 200 μM 3'3'cGAMP for 3 hours, relative to an untreated control. Genes with a fold change ≥2 and false discovery rate ≤10e^{-4} are depicted by black dots. STING is highlighted in red. RNA-seq libraries were prepared from three (2'3' cGAMP) or two (3'3' cGAMP) biological replicates. **(C)** *STING* mRNA levels increase in response to 2'3'cGAMP. Shown are RNA-seq fold changes of *M. brevicollis STING* mRNA after exposure to 2'3'cGAMP (100 μM) or 3'3'cGAMP (200 μM) for three hours, compared to vehicle control. **(D)** Venn diagram comparing the

overlap of genes identified as differentially expressed after treatment with 2'3'cGAMP, 3'3'cGAMP, and *P. aeruginosa* (DEG cutoff: fold change ≥ 3, false discovery rate ≤ $10e^{-4}$). **(E,F)** Representative immunostained *M. brevicollis* demonstrating 2'3'cGAMP stimulates the formation of STING puncta at perinuclear regions. *M. brevicollis* was left untreated (E), or exposed to 100 μM 2'3'cGAMP (F) for 5 hours. Cells were fixed and STING levels and localization were probed using an anti-STING antibody. **(E',F')** Exposure to 2'3'cGAMP results in increased numbers of STING puncta compared to untreated controls. **(E'',F'')** Z-slice images of the plane containing the nucleus 'n' show that STING puncta localize to perinuclear regions. Green: anti-tubulin antibody (flagella and cell body), magenta: anti-STING antibody, blue: Hoechst. Scale bar represents 2 μm.

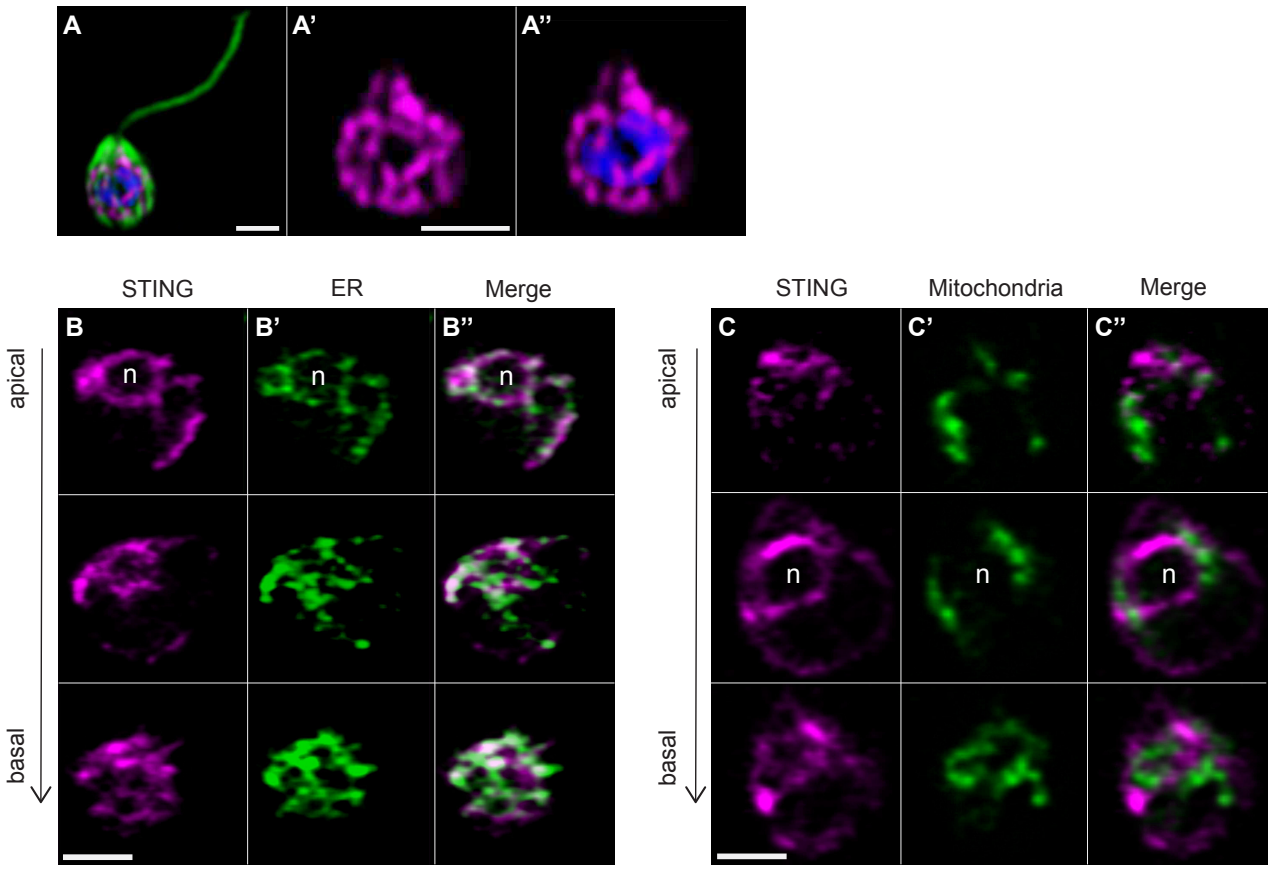

Figure 4. Transfection reveals STING localization to perinuclear and endoplasmic reticulum regions

(A) STING-mTFP localizes to tubule-like structures around the nucleus in cells stably expressing STING-mTFP. Green: anti-tubulin antibody (flagella and cell body), magenta: anti-STING antibody, blue: Hoechst. Scale bar represents 2 μm. **(B,C)** Fluorescent markers and live cell imaging reveal that STING is localized to the endoplasmic reticulum (ER). Cells were co-transfected with STING-mTFP and an mCherry fusion protein that localizes either to the endoplasmic reticulum (B; mCherry-HDEL) or mitochondria (C; Cox4-mCherry)[4]. Cells were recovered in the presence of *Flavobacterium* feeding bacteria for 28 hours after co-transfection, and then live cells were visualized with super-resolution microscopy. Each panel shows Z-slice images of a single representative cell. In confocal Z-slice images, cells are oriented with the apical flagella pointing up, and the nucleus is marked by 'n' when clearly included in the plane of focus. STING colocalized with the ER marker (B''), but not the mitochondrial marker (C''). Scale bar represents 2 μm.

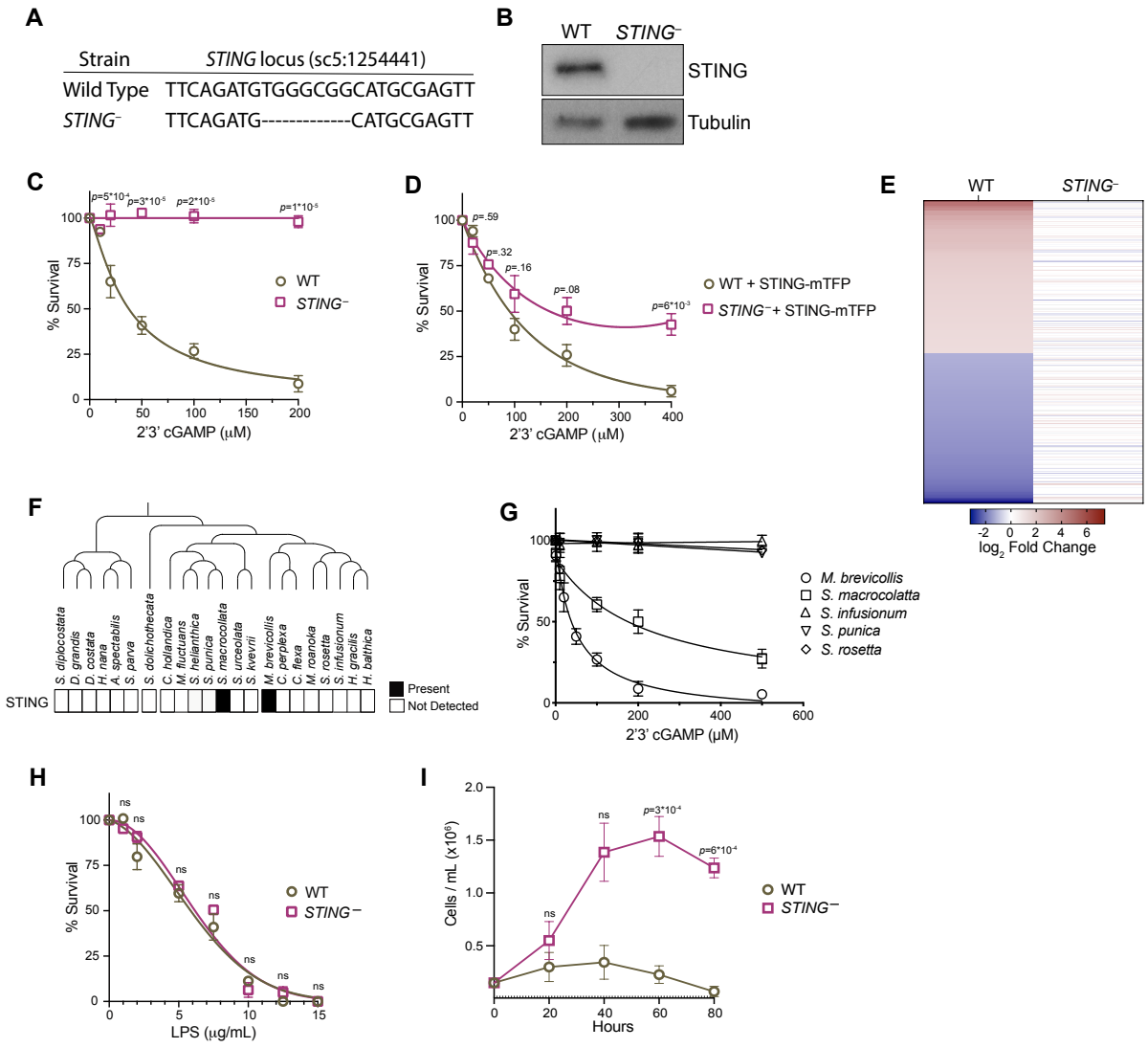

Figure 5. STING mediates responses to 2'3'cGAMP

(A) The genotypes of wild type and genome-edited *STING*⁻ strains at the *STING* locus. **(B)** STING protein is not detectable by immunoblot in *STING*⁻ cells. Shown is a representative blot from three biological replicates. **(C,D)** STING is necessary for 2'3'cGAMP-induced cell death. **(C)** Wild type and *STING*⁻ strains were treated with increasing concentrations of 2'3'cGAMP, and survival was quantified after 24 hours. In contrast to wild type cells, 2'3'cGAMP does not induce cell death in *STING*⁻ cells. Data represent mean +/- SD for four biological replicates. **(D)** Wild type and *STING*⁻ cells were transfected with STING-mTFP, and treated with puromycin to generate stable clonal strains. Stable expression of STING-mTFP in *STING*⁻ cells partially rescued the phenotype of 2'3'cGAMP-induced cell death. Data represent mean +/- SD for three biological replicates. Statistical analysis (multiple unpaired t-tests) was performed in GraphPad software. **(E)** Wild type and *STING*⁻ strains have distinct transcriptional responses to 2'3' cGAMP. Differential expression analysis was performed on wild type

and *STING*$^{-}$ cells treated with 100μM 2'3'cGAMP or a vehicle control for three hours. A heatmap comparing the $\log_2$ fold change of genes identified as differentially expressed (FC ≥2; FDR≤10^{-4}) in wild type cells after 2'3' cGAMP treatment, to their $\log_2$ fold change in *STING*$^{-}$ cells after 2'3' cGAMP treatment. RNA-seq libraries were prepared from two biological replicates. **(F)** Presence of STING in the transcriptomes of diverse choanoflagellate species. Data from Richter et al. 2018[3]. **(G)** Effects of 2'3'cGAMP on different choanoflagellate species. Choanoflagellates were grown to late-log phase, and treated with increasing concentrations of 2'3'cGAMP. Survival was quantified after 24 hours. 2'3'cGAMP only affected the survival of *M. brevicollis* and *S. macrocollata*, the two sequenced choanoflagellate species with a STING homolog. Data represent mean +/- SD for three biological replicates. **(H)** Wild type and *STING*$^{-}$ cells have similar survival responses to LPS, suggesting that STING is not required for mediating a response to LPS. Wild type and *STING*$^{-}$ strains were treated with increasing concentrations of *E. coli* LPS, and survival was quantified after 24 hours. Data represent mean +/- SD for four biological replicates. Statistical analysis (multiple unpaired t-tests) was performed in GraphPad software. **(I)** STING renders *M. brevicollis* more susceptible to *P. aeruginosa*-induced growth inhibition. Wild type and *STING*$^{-}$ cells were exposed to *P. aeruginosa* conditioned media (5% vol/vol), and cell densities were quantified at indicated time points. Data represent mean +/- SD for three biological replicates. Statistical analysis (multiple unpaired t-tests) was performed in GraphPad software. Dashed line indicates limit of detection.

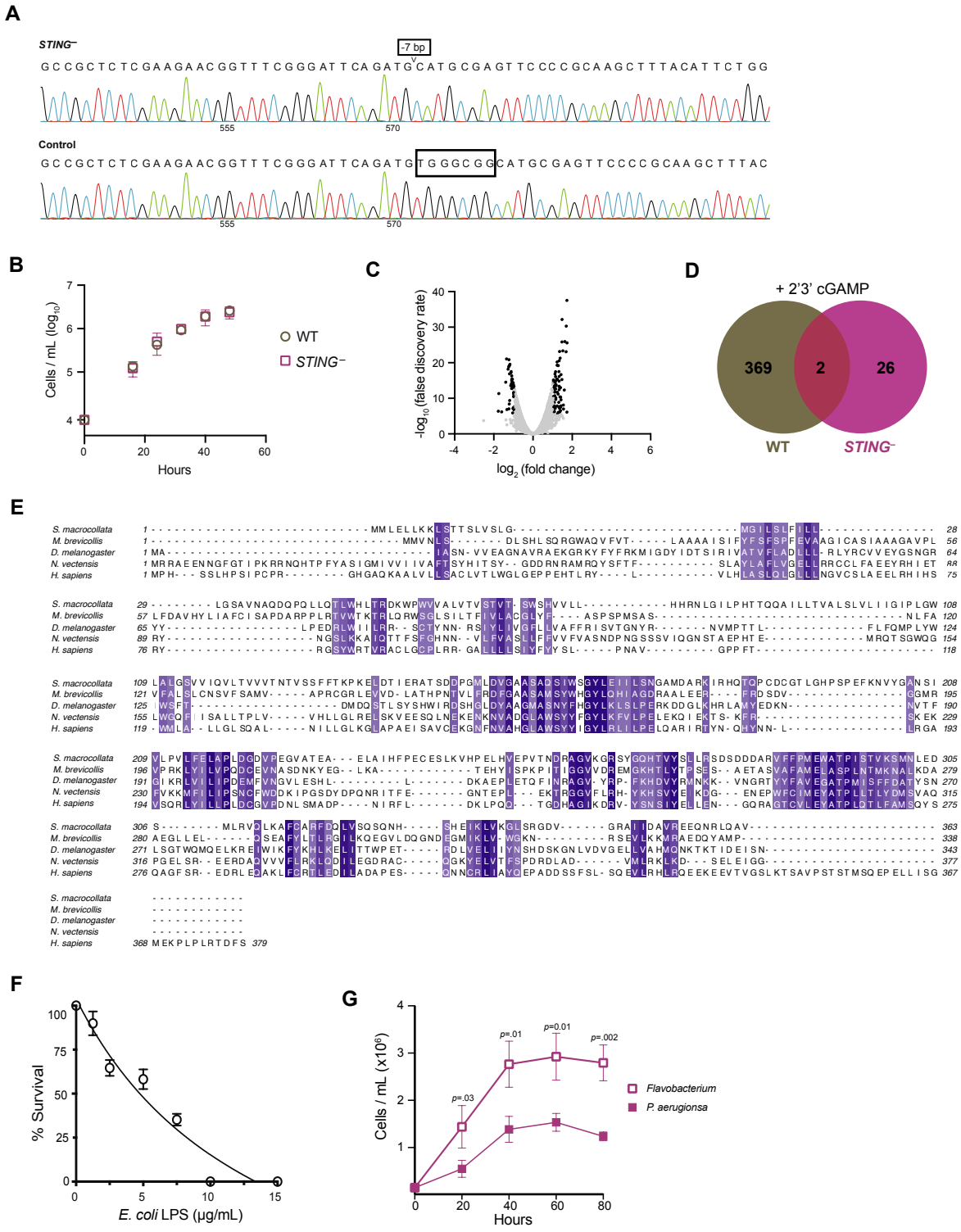

Supplemental Figure 5. Characterizing *STING⁻ M. brevicollis*

(A) Sanger sequences of the consensus genotype at the site of gene editing in wild type and *STING⁻* cells. *STING⁻* cells have a 7 base-pair deletion that leads to premature stop codons. **(B)** Growth curves of wild type and *STING⁻* cells indicate that both strains have

similar growth dynamics. Statistical analysis (multiple unpaired t-tests) was performed in GraphPad software. **(C)** Volcano plot displaying RNA-seq differential expression analysis of *STING*$^{-}$ cells treated with 100 µM 2'3'cGAMP for 3 hours, relative to an untreated control. Genes with a fold change ≥2 and false discovery rate ≤10e^{-4} are depicted by black dots. RNA-seq libraries were prepared from two biological replicates. **(D)** Venn diagram comparing the overlap of genes identified as differentially expressed (FC ≥3; FDR≤10^{-4}) after treatment with 2'3'cGAMP in wild type and *STING*$^{-}$ cells. **(E)** Protein sequence alignment (generated by Clustal Omega multiple sequence alignment) of STING proteins from choanoflagellates *S. macrocollata* and *M. brevicollis* and animals, colored by similarity. **(F)** Dose-response curve of *M. brevicollis* exposed to *E. coli* LPS for 24 hours reveals that LPS leads to cell death in a dose-dependent manner. Data represent mean +/- SD for four biological replicates. **(G)** *STING*$^{-}$ cells were exposed to control *Flavobacterium* or *P. aeruginosa* conditioned medium (5% vol/vol), and cell densities were quantified at indicated time points. Data represent mean +/- SD for three biological replicates. Statistical analysis (multiple unpaired t-tests) was performed in GraphPad software.

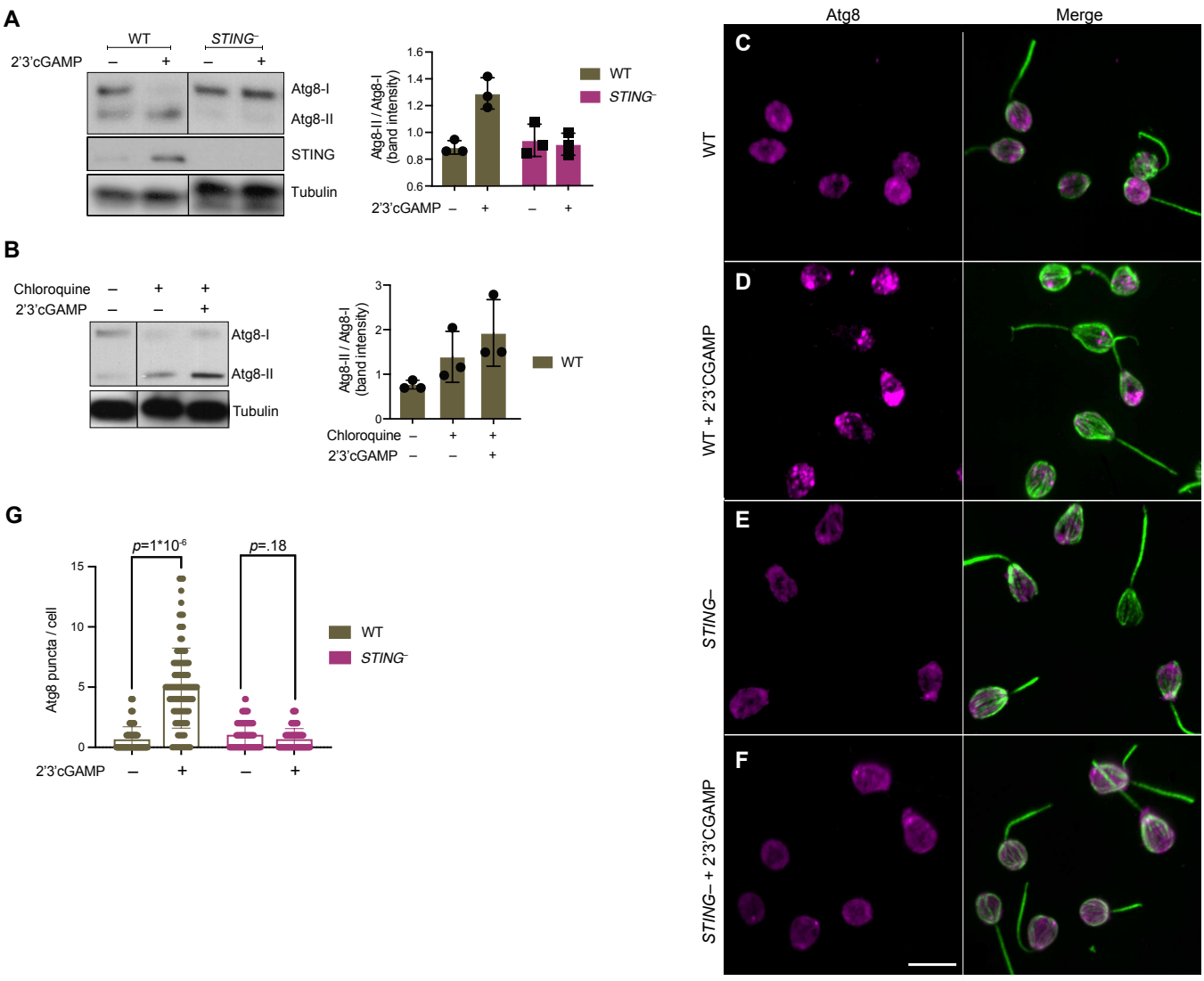

Figure 6. STING mediates 2'3'cGAMP-induced autophagic pathway

(A) 2'3'cGAMP-induced Atg8 lipidation requires STING. WT and *STING*⁻ cells stably expressing mCherry-Atg8 were treated with a vehicle control or 100 μM 2'3'cGAMP for 3 hours, followed by immunoblotting. The band intensity of Atg8-I (unmodified Atg8) and Atg8-II (lipidated Atg8) were quantified for each sample. Relative levels of Atg8 lipidation were assessed by dividing the band intensities of Atg8-II/Atg8-I. Tubulin is shown as loading control. Immunoblot is representative of three biological replicates. **(B)** 2'3'cGAMP induces Atg8 lipidation in chloroquine-treated wild type cells. WT cells stably expressing mCherry-Atg8 were first incubated with 40 mM chloroquine for 6 hours, and then treated with a vehicle control or 100 μM 2'3'cGAMP for 3 hours in the presence of chloroquine, followed by immunoblotting. For each sample, relative levels of Atg8 lipidation were assessed by dividing the band intensities of Atg8-II/Atg8-I. Tubulin is shown as loading control. Immunoblot is representative of three biological

replicates. For a representative immunoblot and quantification of Atg8-II/Atg8-I levels in chloroquine-treated *STING*$^{-}$ cells, refer to Fig. S6B. **(C-G)** STING is required for 2'3'cGAMP-induced autophagosome formation. **(C-F)** WT and *STING*$^{-}$ cells stably expressing mCherry-Atg8 were treated with a vehicle control or 100 μM 2'3'cGAMP for 3 hours, and then fixed and immunostained. **(C,D)** Representative confocal images of wild type cells show that Atg8 puncta accumulate after 2'3'cGAMP treatment. **(E,F)** Representative confocal images of *STING*$^{-}$ cells show that Atg8 remains evenly distributed in the cytoplasm after 2'3'cGAMP treatment. **(G)** The number of Atg8 puncta/cell was quantified for WT and *STING*$^{-}$ cells treated with a vehicle control or 2'3'cGAMP for three hours. Data represent cells quantified from two biological replicates (n=150 cells per treatment group). Statistical analyses (unpaired two-tailed t-tests) were performed in GraphPad software.

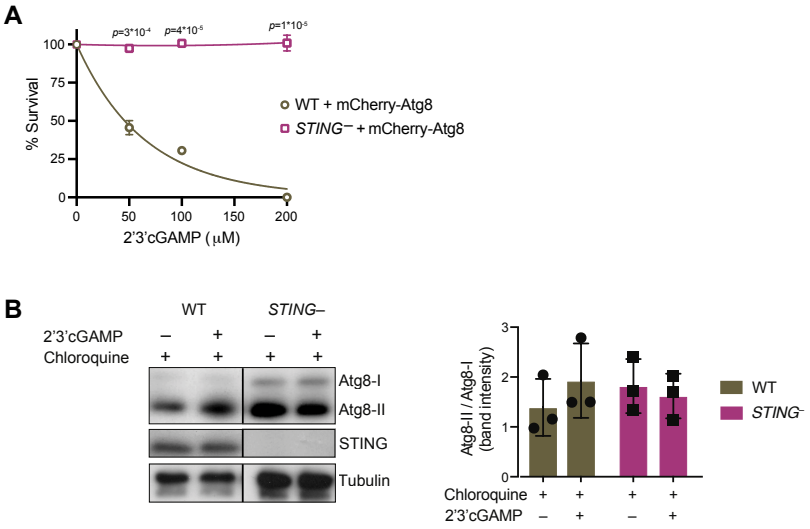

Supplemental Figure 6. STING mediates 2'3'cGAMP-induced autophagic signaling **(A)** Overexpression of mCherry-Atg8 does not alter the susceptibility of wild type and *STING*⁻ strains to 2'3'cGAMP. Wild type and *STING*⁻ strains stably expressing mCherry-Atg8 were treated with increasing concentrations of 2'3'cGAMP, and survival was quantified after 24 hours. Data represent mean +/- SD for two biological replicates. **(B)** 2'3'cGAMP does not induce increased Atg8 lipidation in chloroquine-treated *STING*⁻ cells. *STING*⁻ cells stably expressing mCherry-Atg8 were incubated with 40 mM chloroquine for 6 hours, and then treated with a vehicle control or 100 μM 2'3'cGAMP for 3 hours in the presence of chloroquine, followed by immunoblotting. For each sample, relative levels of Atg8 lipidation were assessed by dividing the band intensities of Atg8-II/Atg8-I. Tubulin is shown as loading control. Immunoblot is representative of three biological replicates.

Table 1. Bacteria screened for pathogenic effects

Bacterium	Pathogenic effects	Reference or details	Source
Aeromonas hyrophila	–	Environmental isolate	This study
Bacillus aquimaris	–	Environmental isolate	This study
Bacillus badius	–	Mouse isolate	Julie Pfeiffer
Bacillus cereus	–	Environmental isolate	This study
Bacillus indicus	–	Environmental isolate	This study
Bacillus marisflavi	–	Environmental isolate	This study
Bacillus pumilus	–	Mouse isolate	Julie Pfeiffer
Bacillus safensis	–	Mouse isolate	Julie Pfeiffer
Bacillus subtilus	–	ATCC 6633	Julie Pfeiffer
Bacteroides acidifaciens	–	Mouse isolate	Julie Pfeiffer
Burkholderia multivorans	–	ATCC 17616	David Greenberg
Campylobacter jejuni GFP	–	DRH3123	David Hendrixson
Deinococcus sp.	–	Environmental isolate	This study
Enterococcus cloacae	–	Mouse isolate	Julie Pfeiffer
Enterococcus faecium	–	Mouse isolate	Julie Pfeiffer
Escherichia coli BW25113	–	Datsenko and Wanner, 2000	David Greenberg
Escherichia coli DH5a GFP	–		David Hendrixson
Escherichia coli ECC-1470	–	Leimbach et al., 2015	Julie Pfeiffer
Escherichia coli K12	–	ATCC 10798	Julie Pfeiffer
Flavobacterium sp.	–	King et al., 2008	Isolated from ATCC PRA-258
Lactobacillis johnsonii	–	Mouse isolate	Julie Pfeiffer
Pseudoalteromonas sp.	–	Environmental isolate	This study
Pseudomonas aeruginosa PA-14	+	Rahm et al., 1995	Andrew Koh
Pseudomonas aeruginosa PAO1	+	ATCC 15692	David Greenberg
Pseudomonas aeruginosa PAO1-GFP	+	Bloemberg et al., 1997	David Greenberg
Pseudomonas granadensis	–	Environmental isolate	This study
Salmonella enterica	–	Mouse isolate	Julie Pfeiffer
Staphylococcus aureus	–	ATCC 23235	Julie Pfeiffer
Staphylococcus sp.	–	Mouse isolate	Julie Pfeiffer
Vibrio alginolyticus	–	Environmental isolate	Kim Orth
Vibrio furnissii	–	Environmental isolate	This study
Vibrio parahaemolyticus	–	Environmental isolate	This study
Vibrio parahaemolyticus	–	Environmental isolate	Kim Orth
Vibrio ruber	–	Environmental isolate	This study
Vibrio sp.	–	Environmental isolate	This study

Table 2. *P. aeruginosa* deletion strains

Strain name	Gene	Putative ORF function	Effects on *M. brevicollis*	
			Truncated Flagellum/ Settling	Cell Death
MPAO1		parent to library stain	+	+
PW5035	pvdE	pyoverdine biosynthesis protein PvdE	+	+
PW5034	pvdE	pyoverdine biosynthesis protein PvdE	+	+
PW1059	exoT	exoenzyme T	+	+
PW3078	toxA	exotoxin A precursor	+	+
PW3079	toxA	exotoxin A precursor	+	+
PW4736	exoY	adenylate cyclase ExoY	+	+
PW4737	exoY	adenylate cyclase ExoY	+	+
PW6886	rhlA	rhamnosyltransferase chain A	+	+
PW6887	rhlA	rhamnosyltransferase chain A	+	+
PW7478	exoS	exoenzyme S	+	+
PW7479	exoS	exoenzyme S	+	+
PW7303	lasB	elastase LasB	+	+
PW7302	lasB	elastase LasB	+	+
PW3252	aprA	alkaline metalloproteinase precursor	+	+
PW3253	aprA	alkaline metalloproteinase precursor	+	+
PW4282	lasA	LasA protease precursor	+	+
PW4283	lasA	LasA protease precursor	+	+

1. Shabalina, S. A. & Koonin, E. V. Origins and evolution of eukaryotic RNA interference. *Trends Ecol Evol* **23**, 578–587 (2008).

2. Richter, D. J. & Levin, T. C. The origin and evolution of cell-intrinsic antibacterial defenses in eukaryotes. *Curr Opin Genet Dev* **58–59**, 111–122 (2019).

3. Richter, D. J., Fozouni, P., Eisen, M. B. & King, N. Gene family innovation, conservation and loss on the animal stem lineage. *Elife* **7**, 946 (2018).

4. King, N. *et al.* The genome of the choanoflagellate Monosiga brevicollis and the origin of metazoans. *Nature* **451**, 783 788 (2008).

5. Brunet, T. & King, N. The Origin of Animal Multicellularity and Cell Differentiation. *Dev Cell* **43**, 124 140 (2017).

6. Richter, D. J. & King, N. The genomic and cellular foundations of animal origins. *Annu Rev Genet* **47**, 509 537 (2013).

7. Leadbeater, B. S. C. *The Choanoflagellates: Evolution, Ecology, and Biology*. (Cambridge University Press, 2015).

8. Dayel, M. J. & King, N. Prey capture and phagocytosis in the choanoflagellate Salpingoeca rosetta. *Plos One* **9**, e95577 (2014).

9. Wu, X. *et al.* Molecular evolutionary and structural analysis of the cytosolic DNA sensor cGAS and STING. *Nucleic Acids Res* **42**, 8243–8257 (2014).

10. Levin, T. C., Greaney, A. J., Wetzel, L. & King, N. The Rosetteless gene controls development in the choanoflagellate S. rosetta. *Elife* **3**, (2014).

11. Ablasser, A. & Chen, Z. J. cGAS in action: Expanding roles in immunity and inflammation. *Science* **363**, eaat8657 (2019).

12. Ahn, J. & Barber, G. N. STING signaling and host defense against microbial infection. *Exp Mol Medicine* **51**, 1–10 (2019).

13. Margolis, S. R., Wilson, S. C. & Vance, R. E. Evolutionary Origins of cGAS-STING Signaling. *Trends Immunol* **38**, 733–743 (2017).

14. Kranzusch, P. J. *et al.* Ancient Origin of cGAS-STING Reveals Mechanism of Universal 2′,3′ cGAMP Signaling. *Mol Cell* **59**, 891 903 (2015).

15. Ishikawa, H. & Barber, G. N. STING is an endoplasmic reticulum adaptor that facilitates innate immune signalling. *Nature* **455**, 674–678 (2008).

16. Sun, L., Wu, J., Du, F., Chen, X. & Chen, Z. J. Cyclic GMP-AMP Synthase Is a Cytosolic DNA Sensor That Activates the Type I Interferon Pathway. *Science* **339**, 786–791 (2013).

17. Burdette, D. L. *et al.* STING is a direct innate immune sensor of cyclic di-GMP. *Nature* **478**, 515–518 (2011).

18. Diner, E. J. *et al.* The Innate Immune DNA Sensor cGAS Produces a Noncanonical Cyclic Dinucleotide that Activates Human STING. *Cell Reports* **3**, 1355–1361 (2013).

19. Gao, P. *et al.* Cyclic [G(2′,5′)pA(3′,5′)p] Is the Metazoan Second Messenger Produced by DNA-Activated Cyclic GMP-AMP Synthase. *Cell* **153**, 1094–1107 (2013).

20. Ablasser, A. *et al.* cGAS produces a 2′-5′-linked cyclic dinucleotide second messenger that activates STING. *Nature* **498**, 380–384 (2013).

21. Moretti, J. *et al.* STING Senses Microbial Viability to Orchestrate Stress-Mediated Autophagy of the Endoplasmic Reticulum. *Cell* **171**, 809-823.e13 (2017).

22. Burroughs, A. M. & Aravind, L. Identification of Uncharacterized Components of Prokaryotic Immune Systems and Their Diverse Eukaryotic Reformulations. *J Bacteriol* **202**, (2020).

23. Alegado, R. A. *et al.* A bacterial sulfonolipid triggers multicellular development in the closest living relatives of animals. *Elife* **1**, e00013 (2012).

24. Brunet, T. *et al.* A flagellate-to-amoeboid switch in the closest living relatives of animals. *Elife* **10**, e61037 (2021).

25. Dayel, M. J. *et al.* Cell differentiation and morphogenesis in the colony-forming choanoflagellate Salpingoeca rosetta. *Dev Biol* **357**, 73 82 (2011).

26. Woznica, A., Gerdt, J. P., Hulett, R. E., Clardy, J. & King, N. Mating in the Closest Living Relatives of Animals Is Induced by a Bacterial Chondroitinase. *Cell* **170**, 1175 1183.e11 (2017).

27. Brunet, T. *et al.* Light-regulated collective contractility in a multicellular choanoflagellate. *Science* **366**, 326–334 (2019).

28. Laundon, D., Larson, B. T., McDonald, K., King, N. & Burkhardt, P. The architecture of cell differentiation in choanoflagellates and sponge choanocytes. *Plos Biol* **17**, e3000226 (2019).

29. Woznica, A. *et al.* Bacterial lipids activate, synergize, and inhibit a developmental switch in choanoflagellates. *Proc National Acad Sci* **113**, 7894 7899 (2016).

30. Ireland, E. V., Woznica, A. & King, N. Synergistic Cues from Diverse Bacteria Enhance Multicellular Development in a Choanoflagellate. *Appl Environ Microb* **86**, (2020).

31. Hake, K. *et al.* Colonial choanoflagellate isolated from Mono Lake harbors a microbiome. (n.d.) doi:10.1101/2021.03.30.437421.

32. Moradali, M. F., Ghods, S. & Rehm, B. H. A. Pseudomonas aeruginosa Lifestyle: A Paradigm for Adaptation, Survival, and Persistence. *Front Cell Infect Mi* **7**, 39 (2017).

33. Mahajan-Miklos, S., Tan, M.-W., Rahme, L. G. & Ausubel, F. M. Molecular Mechanisms of Bacterial Virulence Elucidated Using a Pseudomonas aeruginosa–Caenorhabditis elegans Pathogenesis Model. *Cell* **96**, 47–56 (1999).

34. Pukatzki, S., Kessin, R. H. & Mekalanos, J. J. The human pathogen Pseudomonas aeruginosa utilizes conserved virulence pathways to infect the social amoeba Dictyostelium discoideum. *Proc National Acad Sci* **99**, 3159–3164 (2002).

35. Rahme, L. G. *et al.* Use of model plant hosts to identify Pseudomonas aeruginosa virulence factors. *Proc National Acad Sci* **94**, 13245–13250 (1997).

36. Uribe-Querol, E. & Rosales, C. Control of Phagocytosis by Microbial Pathogens. *Front Immunol* **8**, 1368 (2017).

37. Yoon, S. *et al.* Pseudomonas syringae evades phagocytosis by animal cells via type III effector-mediated regulation of actin filament plasticity. *Environ Microbiol* **20**, 3980–3991 (2018).

38. Klockgether, J. & Tümmler, B. Recent advances in understanding Pseudomonas aeruginosa as a pathogen. *F1000research* **6**, 1261 (2017).

39. Tanaka, Y. & Chen, Z. J. STING Specifies IRF3 Phosphorylation by TBK1 in the Cytosolic DNA Signaling Pathway. *Sci Signal* **5**, ra20–ra20 (2012).

40. Liu, S. *et al.* Phosphorylation of innate immune adaptor proteins MAVS, STING, and TRIF induces IRF3 activation. *Science* **347**, aaa2630 (2015).

41. Zhang, C. *et al.* Structural basis of STING binding with and phosphorylation by TBK1. *Nature* **567**, 394–398 (2019).

42. Abe, T. & Barber, G. N. Cytosolic-DNA-Mediated, STING-Dependent Proinflammatory Gene Induction Necessitates Canonical NF-κB Activation through TBK1. *J Virol* **88**, 5328–5341 (2014).

43. Gui, X. *et al.* Autophagy induction via STING trafficking is a primordial function of the cGAS pathway. *Nature* **567**, 262–266 (2019).

44. Yamashiro, L. H. *et al.* Interferon-independent STING signaling promotes resistance to HSV-1 in vivo. *Nat Commun* **11**, 3382 (2020).

45. Prabakaran, T. *et al.* Attenuation of cGAS-STING signaling is mediated by a p62/SQSTM1-dependent autophagy pathway activated by TBK1. *Embo J* **37**, (2018).

46. Mann, C. C. de O. *et al.* Modular Architecture of the STING C-Terminal Tail Allows Interferon and NF-κB Signaling Adaptation. *Cell Reports* **27**, 1165-1175.e5 (2019).

47. Watson, R. O. *et al.* The Cytosolic Sensor cGAS Detects Mycobacterium tuberculosis DNA to Induce Type I Interferons and Activate Autophagy. *Cell Host Microbe* **17**, 811–819 (2015).

48. Booth, D. S., Szmidt-Middleton, H. & King, N. Choanoflagellate transfection illuminates their cell biology and the ancestry of animal septins. *Mol Biol Cell* **29**, mbcE18080514 (2018).

49. Dobbs, N. *et al.* STING Activation by Translocation from the ER Is Associated with Infection and Autoinflammatory Disease. *Cell Host Microbe* **18**, 157–168 (2015).

50. Booth, D. S. & King, N. Genome editing enables reverse genetics of multicellular development in the choanoflagellate Salpingoeca rosetta. *Elife* **9**, e56193 (2020).

51. Liu, Y. *et al.* Inflammation-Induced, STING-Dependent Autophagy Restricts Zika Virus Infection in the Drosophila Brain. *Cell Host Microbe* **24**, 57-68.e3 (2018).

52. Klionsky, D. J. *et al.* Guidelines for the use and interpretation of assays for monitoring autophagy (4th edition) 1. *Autophagy* **17**, 1–382 (2021).

53. Tanida, I., Minematsu-Ikeguchi, N., Ueno, T. & Kominami, E. Lysosomal Turnover, but Not a Cellular Level, of Endogenous LC3 is a Marker for Autophagy. *Autophagy* **1**, 84–91 (2005).

54. McFarland, A. P. *et al.* Sensing of Bacterial Cyclic Dinucleotides by the Oxidoreductase RECON Promotes NF-κB Activation and Shapes a Proinflammatory Antibacterial State. *Immunity* **46**, 433–445 (2017).

55. Margolis, S. R. *et al.* The STING ligand 2'3'-cGAMP induces an NF-κB-dependent anti-bacterial innate immune response in the starlet sea anemone Nematostella vectensis. *bioRxiv* (2021).

56. Schindelin, J. *et al.* Fiji: an open-source platform for biological-image analysis. *Nat Methods* **9**, 676–682 (2012).

57. Kim, D. *et al.* TopHat2: accurate alignment of transcriptomes in the presence of insertions, deletions and gene fusions. *Genome Biol* **14**, R36 (2013).

58. Liao, Y., Smyth, G. K. & Shi, W. featureCounts: an efficient general purpose program for assigning sequence reads to genomic features. *Bioinformatics* **30**, 923–930 (2014).

59. Robinson, M. D., McCarthy, D. J. & Smyth, G. K. edgeR: a Bioconductor package for differential expression analysis of digital gene expression data. *Bioinformatics* **26**, 139–140 (2010).

60. Peng, D., Kurup, S. P., Yao, P. Y., Minning, T. A. & Tarleton, R. L. CRISPR-Cas9-Mediated Single-Gene and Gene Family Disruption in Trypanosoma cruzi. *Mbio* **6**, e02097-14 (2015).